Discovery of Imidazo[1,5-*c*]imidazol-3-ones: Weakly Basic, Orally Active Factor Xa Inhibitors

Yasuhiro Imaeda,* Takanobu Kuroita, Hiroki Sakamoto, Tetsuji Kawamoto, Mamoru Tobisu,§ Noriko Konishi, Katsuhiko Hiroe, Masaki Kawamura, Toshimasa Tanaka, and Keiji Kubo

Pharmaceutical Research Division, Takeda Pharmaceutical Co., Ltd., 2-17-85, Jusohonmachi, Yodogawa-ku, Osaka 532-8686, Japan

Received December 12, 2007

The coagulation enzyme factor Xa (FXa) has been recognized as a promising target for the development of new antithrombotic agents. We previously found compound **1** to be an orally bioavailable FXa inhibitor in fasted monkeys; however, **1** showed poor bioavailability in rats and fed monkeys. To work out the pharmacokinetic problems, we focused our synthetic efforts on the chemical conversion of the 4-(imidazo[1,2-*a*]pyridin-5-yl)piperazine moiety of **1** to imidazolylpiperidine derivatives (fused and nonfused), which resulted in the discovery of the weakly basic imidazo[1,5-*c*]imidazol-3-one **3q** as a potent and selective FXa inhibitor. Compound **3q** showed favorable oral bioavailability in rats and monkeys under both fasted and fed conditions and antithrombotic efficacy in a rat model of venous thrombosis after oral administration, without a significant increase in bleeding time (unlike warfarin). On the basis of these promising properties, compound **3q** was selected for further evaluation.

Introduction

Abnormal intravascular clot formation is an important factor in a number of cardiovascular diseases such as deep vein thrombosis, pulmonary embolism, myocardial infarction, unstable angina, and ischemic stroke. Agents inhibiting the coagulation cascade, such as heparins, low-molecular-weight heparin, fondaparinux, and vitamin K antagonists (warfarin, acenocoumarol, and fluindione), have been available for the treatment and prevention of these thromboembolic diseases. Vitamin K antagonists prevent the synthesis of vitamin K dependent coagulation factors in the liver and inhibit the activation of blood coagulation leading to thrombus formation. As the only three oral anticoagulants used in a clinical setting, warfarin, acenocoumarol, and fluindione are widely used for the prophylaxis and treatment of venous thromboembolic disease. However, warfarin therapy necessitates a routine blood coagulation test and dose adjustment for each individual because it has substantial drawbacks such as narrow therapeutic dose window, slow onset and offset of action, and interaction with many drugs and food.[1] Despite careful medical treatment, it is difficult to protect patients from the risk of bleeding. Therefore, there is a clear need to develop improved anticoagulants that are orally active, have long duration of action, and have useful in vivo potency without unpredictable or serious bleeding complications.

Factor Xa (FXa[a]) is a key serine protease in the coagulation cascade and essential in the formation of a thrombin, a key mediator of both fibrin formation and platelet activation. It plays an important role in the coagulation network at the common pathway that connects both the tissue factor-activated extrinsic pathway and the surface-activated intrinsic pathway.[2] FXa forms the prothrombinase complex with calcium ion and factor Va, and the complex amplifies the procoagulant action of FXa. FXa acts at an earlier stage in the coagulation cascade than thrombin. Inactivation of FXa by specific inhibitors does not influence preformed thrombin but does effectively prevent the generation of thrombin. Extensive preclinical and clinical proof-of-principal data show that inhibition of FXa is effective in both venous and arterial thrombosis.[3] In animal models, a better therapeutic index (antithrombotic efficacy vs antihemostatic effects, such as bleeding) has been shown for direct FXa inhibitors compared with those for direct thrombin inhibitors and warfarin.[4] On the basis of these data, a cleaner side effect profile would be expected for a FXa inhibitor relative to a thrombin inhibitor in the clinical setting.[3,5]

A variety of direct and low-molecular-weight FXa inhibitors have been described,[6] and orally active FXa inhibitors have been extensively explored.[5d–h] For example, some nonamidine FXa inhibitors such as rivaroxaban[7] and apixaban[8] have been reported to be orally active FXa inhibitors and are under clinical study.

As part of our FXa inhibitor program, we have previously reported that 4-(imidazo[1,2-*a*]pyridin-5-yl)piperazine **1**[9] significantly inhibited human FXa with an IC_{50} of 0.0097 μM, and its in vitro anticoagulant activity PT_2 (the concentration of compound required to double the clotting time in a human prothrombin time (PT) assay) was 1.4 μM. Compound **1** demonstrated good selectivity for FXa versus other serine proteinases and favorable oral bioavailability (BA) in fasted monkeys (BA = 30.5%). Unfortunately, compound **1** showed poor oral bioavailability in fed monkeys, fasted rats, and fed rats. We hoped that the pharmacokinetic behavior might be improved by the modification of the 4-(imidazo[1,2-*a*]pyridin-5-yl)piperazine moiety of compound **1** as the S4 binding element.[6c,8,10]

Our binding model of compound **1** in FXa[9] demonstrated that the 2-hydroxymethylimidazo[1,2-*a*]pyridine moiety formed no salt bridge or hydrogen bond with any amino acid residue in the S4 site, but it did form hydrophobic contacts with the aromatic rings of Tyr99, Phe174, and Trp215 in "the S4 aryl binding site".[11] In particular, the imidazo[1,2-*a*]pyridine ring extends across the face of Phe174 phenyl ring with the favorable $\pi-\pi$ stacking interaction. This result suggests that the 4-(imi-

* To whom correspondence should be addressed. Phone: +81-6-6300-6458. Fax: +81-6-6300-6306. E-mail: Imaeda_Yasuhiro@takeda.co.jp.

§ Current address: Osaka University, 2-1 Yamadaoka, Suita-shi, Osaka 565-0871, Japan.

[a] Abbreviations: FXa, factor Xa; PT, prothrombin time; PT_2, the concentration of compound required to double the clotting time in a human prothrombin time assay; BA, bioavailability; WSC, 1-[3-(dimethylamino)-propyl]-3-ethylcarbodiimide hydrochloride; HOBt, 1-hydroxybenzotriazole hydrate; TFA, trifluoroacetic acid; CDI, 1,1′-carbonyldiimidazole; DBU, 1,8-diazabicyclo[5.4.0]-7-undecene; PDB, Protein Data Bank; CYP, cytochrome P450; t-PA, tissue plasminogen activator.

10.1021/jm701548u CCC: $40.75
Published on Web 05/29/2008

Table 1. In Vitro Activities of Imidazo[1,2-*a*]pyridines **1** and **2**

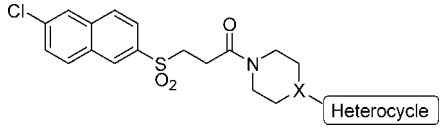

Compd	X	Heterocycle	human FXa IC_{50} (μM)[a]
1	N	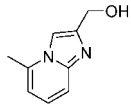	0.0097 (0.0087-0.011)
2	CH	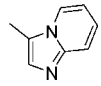	0.012 (0.0099-0.014)

[a] Inhibitory activity against human FXa. IC_{50} values shown are the mean of duplicate measurements. The 95% confidence intervals are shown in parentheses.

dazo[1,2-*a*]pyridin-5-yl)piperazine moiety might not be essential for inhibitory activity, but the hydrophobic contacts at the S4 aryl binding site might be important, so we hypothesized that the imidazo[1,2-*a*]pyridine moiety of **1** as the S4 binding element could be replaced with other basic heteroaromatic rings to improve the pharmacokinetic properties without loss of inhibitory activity. Thus, we initially attempted to replace the piperazine ring with a piperidine ring, shift the substitution position of piperidine ring on the imidazo[1,2-*a*]pyridine ring, and remove the 2-hydroxymethyl group to modulate the physiochemical profiles. This initial effort resulted in the discovery of 4-(imidazo[1,2-*a*]pyridin-3-yl)piperidine **2** as an interesting new lead (Table 1). The quite similar FXa inhibitory activities between **1** and **2** (IC_{50} = 0.0097 μM for **1** vs 0.012 μM for **2**) opened up the possibility to explore imidazolylpiperidine derivatives (fused and nonfused). There are no reports on FXa inhibitors bearing an imidazolylpiperidine moiety. Therefore, we were prompted to design and synthesize new imidazole and bicyclic imidazole derivatives **3** (Figure 1) in an attempt to further improve the pharmacokinetic properties.

In this paper, we describe the synthesis and structure−activity relationships for **3** and show that weakly basic imidazo[1,5-*c*]imidazol-3-one **3q** is a potent and selective direct FXa inhibitor with excellent in vivo activity and favorable oral bioavailability unaffected by food intake, thus making it a promising drug candidate for further evaluation.[12]

Chemistry

The synthesis of imidazo[1,2-*a*]pyridine **2** and tetrahydroimidazo[1,2-*a*]pyridine **3a** is shown in Scheme 1. The key intermediate piperidine **7a** was prepared by condensation of bromoacetaldehyde **4**[13] and 2-aminopyridine **5** followed by removal of the Boc group. Catalytic hydrogenation of imidazo[1,2-*a*]pyridine **6** using PtO_2 followed by deprotection of the Boc group gave tetrahydroimidazo[1,2-*a*]pyridine **7b**. Piperidines **7a** and **7b** were coupled with 3-(6-chloronaphthalen-2-yl)sulfonylpropionic acid **8**[14] using 1-[3-(dimethylamino)propyl]-3-ethylcarbodiimide hydrochloride (WSC) and 1-hydroxybenzotriazole hydrate (HOBt) and successively treated with concentrated HCl to give the desired amides **2** and **3a**.

4-(Imidazol-5(4)-yl)piperidines **3b**−**e** were synthesized as shown in Scheme 2. Piperidines **9a** and **9b**[15,16] were coupled with carboxylic acid **8** to give the desired amides **3b** and **3c**. Regioselective N-methylation to obtain 1-methylimidazoles **3d** and **3e** was carried out by N-tritylation on the less hindered nitrogen atom in the imidazole rings of **3b** and **3c**, subsequent formation of the quaternary imidazolium salt using iodomethane, and finally removal of the trityl group under acidic conditions.[16]

4-(Imidazol-1-yl)piperidines **3f**−**i** were prepared by the method outlined in Scheme 3. The displacement reaction of mesylate **11** with imidazoles **12a** and **12b** gave piperidines **13a** and **13b**. Removal of the Boc group from piperidines **13a**−**d**[17] followed by coupling with carboxylic acid **8** afforded amides **3f**−**i**.

The synthesis of 4-(imidazol-2-yl)piperidines **3j** and **3k** is depicted in Scheme 4. Removal of the Boc group from piperidines **14**[17] and **15**, prepared by methylation of **14**, followed by coupling with carboxylic acid **8** gave the desired amides **3j** and **3k**.

Alkylene-linked imidazoles **3l**−**o** were synthesized as described in Scheme 5. Intermediates **17a**−**d** were prepared from 2-methylimidazole by alkylation with 4-(bromoalkyl)piperidine **16a**−**d**[18] in the presence of sodium hydride. Removal of the Boc group from **17a**−**c** followed by condensation with carboxylic acid **8** and treatment with 4 M HCl in EtOAc gave the desired amides **3l**−**n**. Removal of the Boc group from **17d** followed by coupling with carboxylic acid **8** gave amide **3o**.

The synthesis of alkylene-linked imidazole **3p** was shown in Scheme 6. Alkylation of 2-methylimidazole with **18**[19] in the presence of sodium hydride gave amide **19**. Treatment with trifluoroacetic acid (TFA) and subsequent reduction of the amide bond with lithium aluminum hydride afforded piperazine **20**, which was condensed with carboxylic acid **8** to give the desired amide **3p**.

Imidazo[1,5-*c*]imidazol-3-ones **3q** and **3r** were synthesized as follows (Scheme 7). Reductive amination of imidazolecarbaldehydes **22a** and **22b** with 4-aminopiperidine **21** gave aminomethylimidazole **23a** and **23b**. Cyclization of **23a** or **23b** using 1,1′-carbonyldiimidazole (CDI) and 1,8-diazabicyclo[5.4.0]-7-undecene (DBU) afforded imidazo[1,5-*c*]imidazol-3-one **24a** or **24b**. Removal of the Boc group from **24a** and **24b** with concentrated HCl and successive condensation with **8** provided the corresponding amides **3q** and **3r**.

The synthesis of imidazo[1,5-*c*]imidazol-3-one **3s**, a piperazine analogue of **3q**, is depicted in Scheme 8. Hydrazone **26**, prepared from hydrazine **25**[18] and **22a**, was reduced with borane−tetrahydrofuran complex and subsequently treated with hydrochloric acid for decomposition of aminopiperazine−borane complex to give hydrazine **27**. Cyclization of **27** with CDI afforded imidazo[1,5-*c*]imidazol-3-one **28**, which was converted into piperazine **29** by palladium-catalyzed debenzylation with ammonium formate. Coupling of carboxylic acid **8** with piperazine **29** gave the desired amide **3s**.

Results and Discussion

The compounds thus synthesized were evaluated in vitro for inhibitory potency against human FXa, expressed as IC_{50} values, and for their activity in the prolongation of human PT, expressed as PT_2. To estimate the oral bioavailability of these compounds, the ex vivo PT prolonging activity was also determined 1 h after oral administration to mice at a dose of 30 mg/kg and expressed as ratios of the PT of the compound in treatment mice to that of the untreated group.

The activities of 4-(imidazol-5(4)-yl)piperidine derivatives are shown in Table 2. Tetrahydroimidazo[1,2-*a*]pyridine **3a** exhibited slightly less potent FXa inhibitory activity (IC_{50} = 0.023 μM for **3a** vs 0.012 μM for **2**) compared to **2**, while **3a** showed more potent in vitro anticoagulant activity compared to **2** (PT_2 = 0.48 μM for **3a** vs 2.2 μM for **2**). This result suggests that

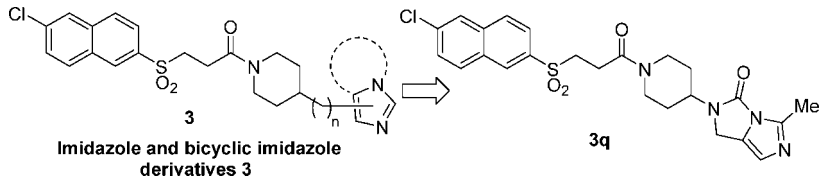

Figure 1

Scheme 1[a]

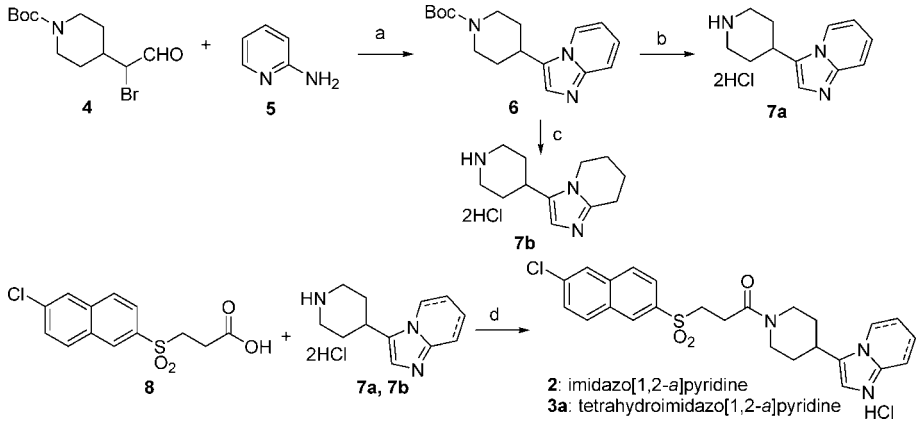

[a] Reagents and conditions: (a) EtOH, reflux, 60%; (b) concd HCl, 91%; (c) (1) H_2, PtO_2, (2) concd HCl, 95%; (d) (1) WSC, HOBt, DBU, Et_3N, (2) concd HCl, 81−82%.

Scheme 2[a]

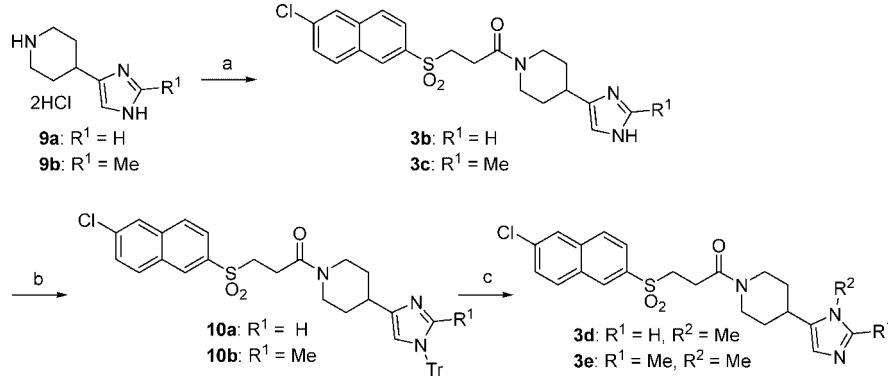

[a] Reagents and conditions: (a) **8**, WSC, HOBt, DBU, Et_3N, 50−91%; (b) TrCl, Et_3N, 60−100%; (c) (1) MeI, (2) AcOH, 48−76%.

Scheme 3[a]

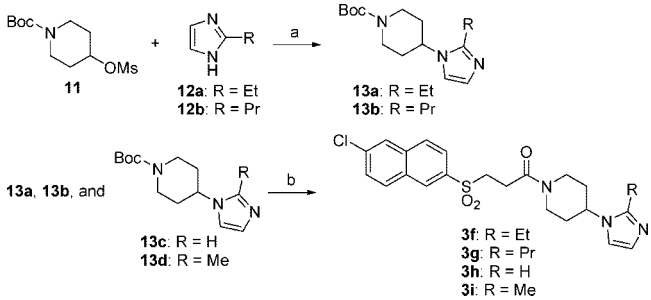

[a] Reagents and conditions: (a) K_2CO_3 or NaH, 3−11%; (b) (1) concd HCl, (2) **8**, WSC, HOBt, DBU, Et_3N, 66−98%.

Scheme 4[a]

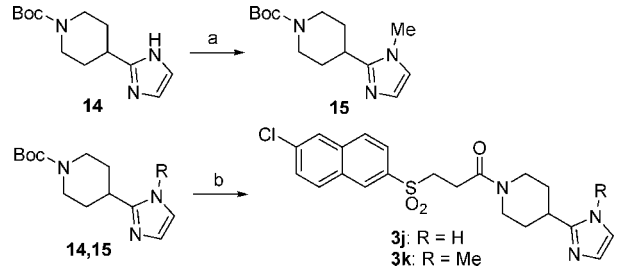

[a] Reagents and conditions: (a) MeI, NaH, 100%; (b) (1) concd HCl, (2) **8**, WSC, HOBt, DBU, Et_3N, 54−70%.

the improvement in anticoagulant potency of **3a** may be attributed to lower lipophilicity (log D = 2.2 for **3a**, 2.5 for **2** at pH 7.4)[20] and increased basicity (pK_a = 8.2 for **3a**, 5.9 for **2**).[21] Thus, we speculated that the lipophilicity and basicity of the S4 binding element influenced the in vitro anticoagulant activities of these compounds.[22] The 1-methylimidazoles **3d** and **3e** are equipotent to tetrahydroimidazo[1,2-*a*]pyridine **3a** in human FXa inhibitory potency and in vitro anticoagulant activity. On the other hand, compounds **3b** and **3c** (R^1 = H) are slightly less potent than **3d** and **3e**. The basicity and the lipophilicity of **3c** (pK_a = 7.9, log D = 2.0 at pH 7.4) are similar to those of **3d** and **3e** (i.e., pK_a = 8.2, log D = 2.0 at pH 7.4 for **3e**). This result suggests that the existence of a free hydrogen atom on either nitrogen atom in the imidazole rings of **3b** and **3c** might interrupt the interaction between the S4 site of FXa

Scheme 5[a]

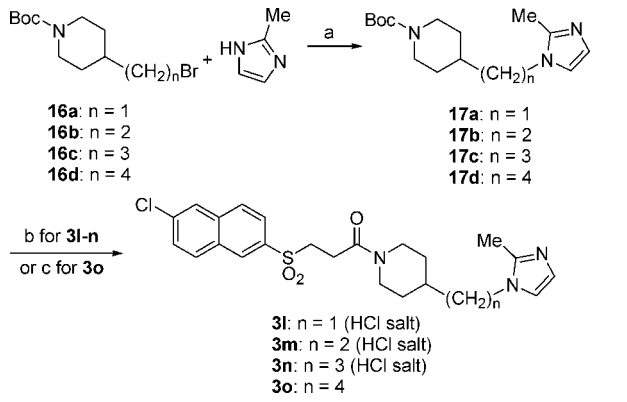

[a] Reagents and conditions: (a) NaH, 7−100%; (b) (1) concd HCl, (2) **8**, WSC, HOBt, DBU, Et_3N, (3) 4 M HCl/EtOAc, 53−74%; (c) (1) concd HCl, (2) **8**, WSC, HOBt, DBU, Et_3N, 15%.

Scheme 6[a]

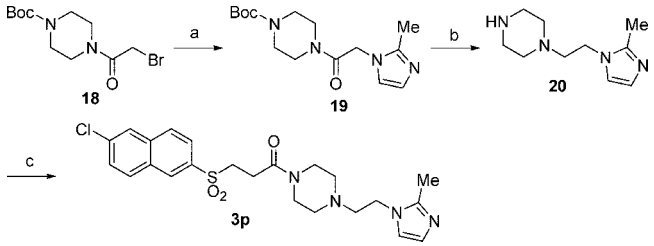

[a] Reagents and conditions: (a) 2-methylimidazole, NaH, 68%; (b) (1) TFA, (2) $LiAlH_4$, 40%; (c) **8**, WSC, HOBt, Et_3N, 2%.

and the imidazole ring. As a result, the 1-methylimidazole moiety of **3d** and **3e** was found to be a new effective S4 binding element.

To investigate the influence of the substitution position of the 4-piperidine moiety on the imidazole ring, some 4-(imidazol-1-yl)piperidines (**3f**−**i**) and 4-(imidazol-2-yl)piperidines (**3j** and **3k**) were examined and the results are shown in Table 3. Among them, the 2-methyl (**3i**) and 2-ethyl (**3f**) derivatives showed the most potent anticoagulant activities. The FXa inhibitory activity of 4-(2-methylimidazol-1-yl)piperidine **3i** was slightly weaker than that of the regioisomer 4-(1-methylimidazol-5-yl)piperidine **3d**. Compound **3j**, lacking an N-substituent, exhibited notably less potent in vitro activity. In comparison to **3i**, 4-(1-methylimidazol-2-yl)piperidine **3k** inhibited FXa slightly more potently, whereas its anticoagulant activity was slightly less potent. The FXa inhibitory activity, basicity, and lipophilicity of **3k** ($IC_{50} = 0.056$ μM, $pK_a = 6.9$, log $D = 2.1$ at pH 7.4) are similar to those of **3d** ($IC_{50} = 0.056$ μM, $pK_a = 7.2$, log $D = 2.0$), but **3k** was nevertheless less potent with respect to in vitro anticoagulant activity than **3d** ($PT_2 = 2.1$ for **3k** vs 0.49 μM for **3d**). These data suggested that the position of the imidazole ring nitrogen might be more important for in vitro anticoagulant activity than basicity or lipophilicity for these inhibitors. 4-(Imidazol-5-yl)piperidines **3d** and **3e** were found to be the most potent FXa inhibitors in our 4-(imidazolyl)piperidine series.

In our effort to achieve further enhancement of FXa potency, a molecular modeling study of **2** and **3a** was carried out using the program GOLD[23] and the X-ray structure of FXa reported by Sanofi-Aventis for an inhibitor complex (PDB code 1EZQ)[24] (Figure 2). In this model, the imidazo[1,2-*a*]pyridine ring of **2** (orange) and the tetrahydroimidazo[1,2-*a*]pyridine ring of **3a** (white) are located at the S4 aryl binding site of FXa.[25] In this site, an open space around the imidazole rings (yellow circle) was found to be available to accommodate structural modifications and the imidazole rings appeared able to shift into the deeper S4 aryl binding site as shown in Figure 2 (yellow arrow). Thus, we designed our next set of compounds to incorporate varied alkylene chains between the imidazole ring and the piperidine ring, hoping to enhance the interaction with this site.

The in vitro anti-FXa and PT prolonging activities obtained for the compounds thus synthesized, of type **3i**, are listed in Table 4. Ethylene-linked imidazole **3m** (FXa $IC_{50} = 0.037$ μM) was found to be more potent than the other alkylene-linked imidazoles **3l**, **3n**, **3o**, and original compound **3i**. The in vitro anticoagulant activity of **3m** was equipotent to that of **3i** ($PT_2 = 0.91$ for **3m** vs 0.99 μM for **3i**). The in vitro activity of piperazine **3p**, which has an ethylene linker, was approximately equal to that of piperidine **3m**. A molecular modeling study of **3i**, **3m**, and **3p** was carried out using the same model described above (Figure 3). In this model, the imidazole ring of **3i** (orange) and the imidazolylethyl groups of **3m** (white) and **3p** (green) are located at the S4 aryl binding site of FXa (yellow circle). In this site, the imidazolylethyl groups of **3m** and **3p** appeared to occupy the deeper S4 aryl binding site more than the imidazole ring of **3i**. Because **3m** and **3p** were found to be more potent FXa inhibitors than **3i**, we speculated that the imidazolylethyl group in **3m** and **3p** might contribute to the enhancement of interaction with the S4 site of FXa compared to the imidazolyl group of **3i**.

Compound **3m** was considered to have poor oral bioavailability in mice, as discussed in more detail below, which might be ascribed to the flexible ethylene linker. We expected that lowering the flexibility of the ethylene linker by cyclization with the imidazole ring might improve oral bioavailability because of a decrease in the number of rotatable bonds.[26] Moreover, we attempted to lower the basicity of **3m** by introduction of an electron-withdrawing carbonyl group onto the imidazole nitrogen atom as a component for cyclization because the basicity of compound **1** ($pK_a = 5.6$), which showed favorable oral bioavailability in mice and fasted monkeys, was lower than for compounds that had poor oral bioavailability in mice ($pK_a >$ 7.1 for **3a**, **3d**, **3e**, and **3m**), as discussed in more detail below.[27] Hence, we designed and synthesized the weakly basic bicyclic imidazo[1,5-*c*]imidazol-3-one moiety as a novel S4 binding element by introduction of an electron-withdrawing carbonyl group on the imidazole nitrogen atom as a component for cyclization. The imidazo[1,5-*c*]imidazol-3-one derivatives have not been reported previously; however, the chemical synthesis is simple and robust. The results of imidazo[1,5-*c*]imidazol-3-ones **3q**−**s** ($pK_a = 5.0$−5.4) are shown in Table 5. Interestingly, compounds **3q** and **3r** showed more potent FXa inhibitory activity than imidazolylethylpiperidine **3m**, with IC_{50} values in the single-digit nanomolar range (FXa $IC_{50} = 0.0048$−0.0053 μM for **3q** and **3r** vs 0.037 μM for **3m**). Piperazine **3s** showed potent FXa inhibitory activity ($IC_{50} = 0.0069$ μM) comparable to that of the corresponding piperidine **3q**. Surprisingly, in vitro anticoagulant activities of **3q**−**s** were similar to that of **3m** ($PT_2 = 0.61$−1.2 μM for **3q**−**s** vs 0.91 μM for **3m**) despite the unambiguous difference in their FXa inhibitory activities. The reason for these results could not be explained in terms of lipophilicity (log $D = 2.1$−2.5 for **3q**−**s**, 2.2 for **3m** at pH 7.4); however, it might be attributed to the difference in basicity ($pK_a = 5.0$−5.4 for **3q**−**s**, 7.9 for **3m**) caused by the existence of a carbonyl group on the imidazo[1,5-*c*]imidazol-3-one ring.

The ex vivo PT prolongation activity after oral administration in mice and cytochrome P450 (CYP) 3A4[28] inhibitory activities of the more potent compounds described above are shown in

Scheme 7[a]

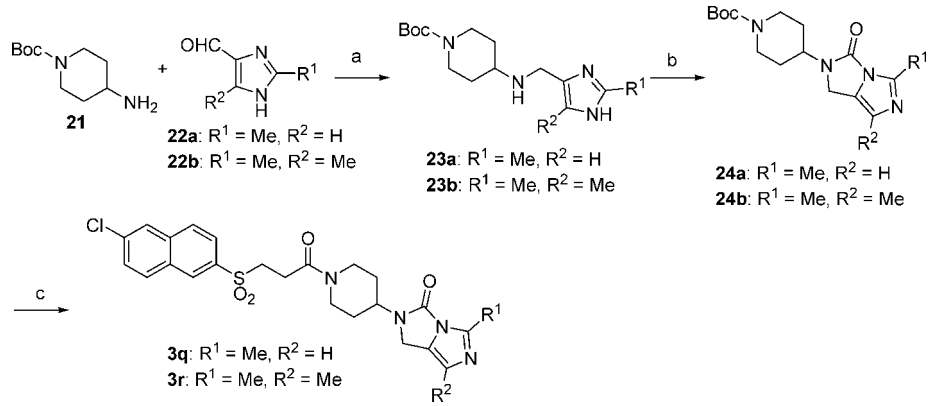

[a] Reagents and conditions: (a) $NaBH(OAc)_3$, AcOH, 100%; (b) CDI, DBU, 77−97%; (c) (1) concd HCl; (2) **8**, WSC, HOBt, Et_3N, 50−73%.

Scheme 8[a]

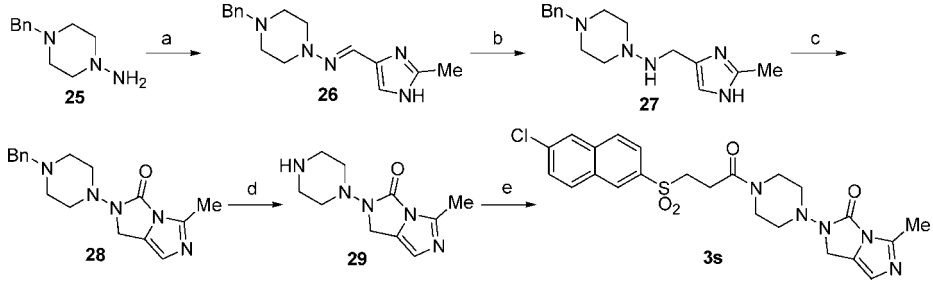

[a] Reagents and conditions: (a) **22a**, 88% (b) (1) BH_3·THF, (2) 6 M HCl, 100%; (c) CDI, DBU, 65%; (d) HCO_2NH_4, 10% Pd/C, 93%; (e) **8**, WSC, HOBt, Et_3N, 76%.

Table 2. In Vitro Activities of 4-(Imidazol-5(4)-yl)piperidines **3a−e**

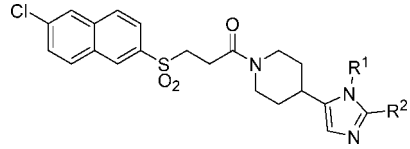

compd	R^1	R^2	human FXa, IC_{50} (μM)[a]	human PT, PT_2 (μM)[b]	log D[c]	pK_a[d]
2			0.012 (0.0099−0.014)	2.2	2.5	5.9
3a	−$(CH_2)_4$−		0.023 (0.022−0.024)	0.48	2.2	8.2
3b	H	H	0.17 (0.15−0.20)	3.0	2.0	6.9
3c	H	Me	0.12 (0.10−0.14)	2.5	2.0	7.9
3d	Me	H	0.056 (0.052−0.059)	0.49	2.0	7.2
3e	Me	Me	0.031 (0.028−0.034)	0.56	2.0	8.2

[a] Inhibitory activity against human FXa. IC_{50} values shown are the mean of duplicate measurements. The 95% confidence intervals are shown in parentheses. [b] PT (prothrombin time) is defined as the concentration of compound required to double the time to clot formation in the PT assay. PT_2 values shown are the mean of duplicate measurements. [c] Measured at pH 7.4. [d] Measured using a titration method.

Table 6. Tetrahydroimidazo[1,2-*a*]pyridine **3a**, imidazolylpiperidine derivatives **3d**, **3e**, and **3i**, and imidazolylethyl derivatives **3m** and **3p** exhibited low ex vivo mouse PT ratios, and so these compounds were judged to have poor oral bioavailability in mice. On the other hand, imidazo[1,5-*c*]imidazol-3-one derivatives **3q−s** showed significant mouse PT prolonging activities and thus appeared to have favorable oral bioavailability in mice. These results support our assumption that lowering the flexibility and basicity of the S4 binding element could dramatically improve oral bioavailability. 5-Methylimidazo[1,5-*c*]imidazol-3-ones **3q** and **3s** showed considerably weak CYP3A4 inhibitory activity at 10 μM, whereas 5,7-dimethylimidazo[1,5-*c*]imidazol-3-one **3r** inhibited CYP3A4 significantly. On the basis of their ex vivo PT prolongation activities in mice and their weak CYP3A4 inhibitory potencies, compounds **3q** and **3s** were selected for evaluation in cynomolgus monkeys.

In order to estimate the oral bioavailability in fasted and fed monkeys, the ex vivo PT prolonging activities in cynomolgus monkeys were determined for **3q** and **3s**. After a 3 mg/kg oral dose, both compounds prolonged PT significantly with long duration of action under fasted conditions (Figure 4A). Under fed conditions, compound **3q** showed as potent a PT prolonging activity as under fasted conditions, whereas compound **3s** showed prolonged PT to a lesser extent following oral dosing (Figure 4B).

Since many trypsin-like proteases have essential physiological functions,[29] an important consideration for the development of FXa inhibitors is the ability of the molecule to bind selectively. Compound **3q** displayed >3000-fold selectivity for FXa versus several coagulation (thrombin), fibrinolytic (plasmin, tissue plasminogen activator (t-PA)), and digestive enzymes (trypsin) (Table 7).

Table 3. In Vitro Activities of 4-(Imidazol-1-yl)piperidines **3f−i** and 4-(Imidazol-2-yl)piperidines **3j** and **3k**

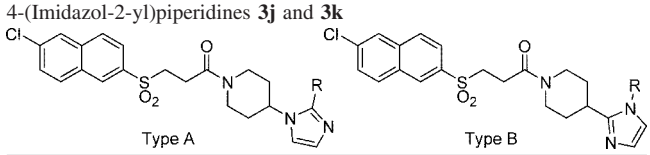

compd	type	R	human FXa, IC_{50} (μM)[a]	human PT, PT_2 (μM)[b]
3d			0.056 (0.052−0.059)	0.49
3f	A	Et	0.16 (0.14−0.17)	1.0
3g	A	Pr	0.23 (0.19−0.28)	2.0
3h	A	H	1.4 (1.3−1.6)	7.0
3i	A	Me	0.17 (0.16−0.18)	0.99
3j	B	H	1.6 (1.4−1.8)	>10
3k	B	Me	0.056 (0.053−0.060)	2.1

[a] Inhibitory activity against human FXa. IC_{50} values shown are the mean of duplicate measurements. The 95% confidence intervals are shown in parentheses. [b] PT (prothrombin time) is defined as the concentration of compound required to double the time to clot formation in the PT assay. PT_2 values shown are the mean of duplicate measurements.

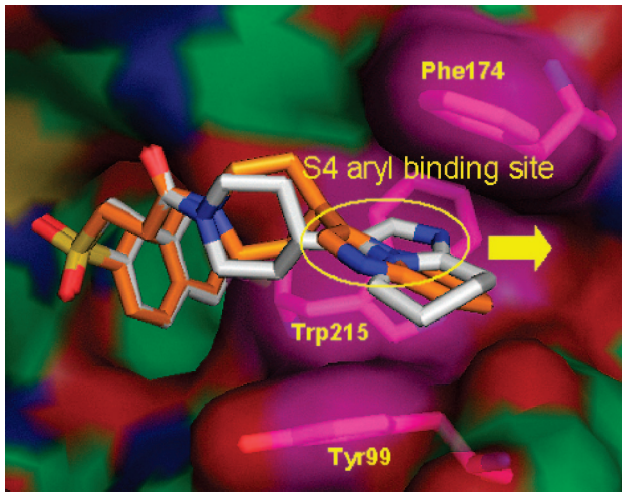

Figure 2. Superimposed binding model of compounds **2** (orange) and **3a** (white) in FXa.

Table 4. In Vitro Activities of Alkylene-Linked Imidazoles **3l−p**

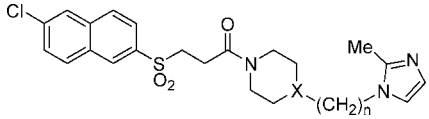

compd	*n*	X	human FXa, IC_{50} (μM)[a]	human PT, PT_2 (μM)[b]
3i	0	CH	0.17 (0.16−0.18)	0.99
3l	1	CH	0.91 (0.85−0.98)	7.7
3m	2	CH	0.037 (0.036−0.039)	0.91
3n	3	CH	0.46 (0.42−0.49)	>10
3o	4	CH	0.30 (0.29−0.32)	>10
3p	2	N	0.054 (0.051−0.057)	0.99

[a] Inhibitory activity against human FXa. IC_{50} values shown are the mean of duplicate measurements. The 95% confidence intervals are shown in parentheses. [b] PT (prothrombin time) is defined as the concentration of compound required to double the time to clot formation in the PT assay. PT_2 values shown are the mean of duplicate measurements.

The pharmacokinetic profile of compound **3q** was evaluated after single intravenous and oral administration to male Sprague−Dawley rats and male cynomolgus monkeys. As illustrated in Table 8, **3q** displayed favorable oral bioavailability after oral administration at a dose of 3 mg/kg in fed rats (24%) and monkeys (46%), respectively. As shown in Table 9, the values of C_{max} in fasted animals were higher than those in the fed state, whereas the values of AUC_{0-24h} in the fasted and fed states were almost the same. These results indicated that **3q** has favorable oral bioavailability in rats and monkeys without significant influence from food intake. Furthermore, **3q** showed considerably weak inhibition of CYP isoforms at 10 μM (CYP2C8, 35% inhibition;[30] CYP2C9, 0% inhibition;[30] CYP2D6, 5% inhibition[31]).

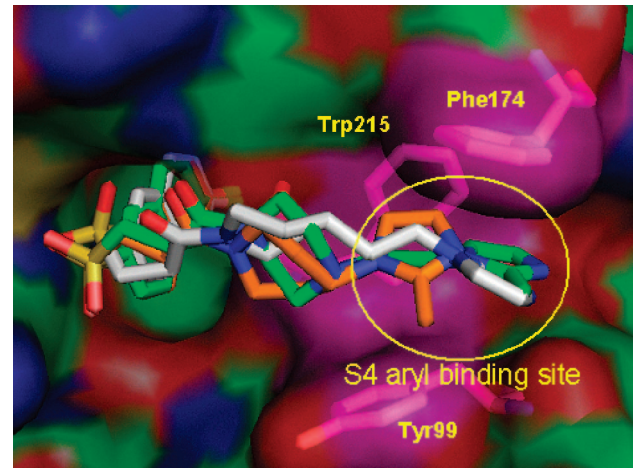

Figure 3. Superimposed binding model of compounds **3i** (orange), **3m** (white), and **3p** (green) in FXa.

In order to evaluate the efficacy of compound **3q** as an oral anticoagulant agent, it was tested in a rat model of venous thrombosis (Figure 5). Compound **3q** at doses of 1, 3, and 10 mg/kg po reduced thrombus formation by 32%, 53%, and 86%, respectively. On the other hand, warfarin, an orally active antithrombotic agent, reduced thrombus formation by 82% at 1 mg/kg po; however, its antithrombotic effect was reduced remarkably at 0.3 mg/kg po.

The bleeding times for compound **3q** and warfarin were determined in rats and are shown in Table 10. Compound **3q** at 30 mg/kg po had little effect on the bleeding time, and a higher dose (100 mg/kg, po) tended to prolong bleeding time to 2.3 times the control value. Meanwhile, warfarin at 1 mg/kg po (minimal dose preventing thrombus formation in rat model) showed significant prolongation of bleeding time to 4.4 times the control value. These results suggest that compound **3q** could achieve antithrombotic efficacy without a significant increase in bleeding time in rats, unlike warfarin. On the basis of its potency, selectivity, pharmacokinetic profile, and in vivo efficacy, compound **3q** was selected for further evaluation.

To predict the binding mode of compound **3q**, a molecular modeling study was carried out using the program GOLD and the X-ray structure of FXa reported by Sanofi-Aventis for an inhibitor complex (PDB code 1EZQ)[24] (Figure 6). In the model, the imidazo[1,5-*c*]imidazol-3-one moiety forms no salt bridge with the carboxyl group of Asp189 at the bottom of the S1 pocket, while the 6-chloronaphthyl group is deeply buried inside the hydrophobic S1 region with the chlorine atom pointing toward the center of the Tyr228 aromatic ring.[7,11b,22b,32] Compound **3q** represents a related example in FXa inhibition, wherein a basic group thought to be essential in forming a crucial salt bridge with Asp189[6d,24] can be eliminated and replaced by a neutral group capable of providing high affinity for the enzyme. A hydrogen bonding interaction between the amide carbonyl group in **3q** and the backbone amide nitrogen of Gly219 is observed. Recently, other researchers have reported that the important interaction for high affinity to FXa is not an ionic interaction with Asp189 but hydrogen bonding interactions with the carbonyl groups in the amide linkages of Gly216 and/or Gly219.[24,32c,33] The imidazo[1,5-*c*]imidazol-3-one moiety is

Table 5. In Vitro Activities of Imidazo[1,5-*c*]imidazol-3-ones **3q**−**s**

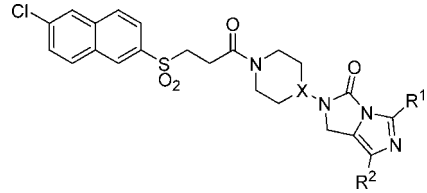

compd	R^1	R^2	X	human FXa, IC_{50} (μM)[a]	human PT, PT_2 (μM)[b]	log D[c]	pK_a[d]
3m				0.037 (0.036−0.039)	0.91	2.2	7.9
3q	Me	H	CH	0.0048 (0.0046−0.0051)	1.0	2.3	5.0
3r	Me	Me	CH	0.0053 (0.0048−0.0059)	1.2	2.5	5.4
3s	Me	H	N	0.0069 (0.0061−0.0078)	0.61	2.1	5.0

[a] Inhibitory activity against human FXa. IC_{50} values shown are the mean of duplicate measurements. The 95% confidence intervals are shown in parentheses. [b] PT (prothrombin time) is defined as the concentration of compound required to double the time to clot formation in the PT assay. PT_2 values shown are the mean of duplicate measurements. [c] Measured at pH 7.4. [d] Measured using a titration method.

Table 6. In Vitro and Ex Vivo Activities of Potent FXa Inhibitors

compd	in vitro: human PT PT_2 (μM)[a]	in vitro: mouse PT PT_2 (μM)[a]	ex vivo, mouse PT Ratio[b]	CYP3A4, % inhibition at 10 μM
3a	0.48	3.0	1.1	42
3d	0.49	2.7	1.2	82
3e	0.56	3.4	1.2	25
3i	0.99	3.3	1.1	34
3m	0.91	1.7	1.1	38
3p	0.99	2.1	1.1	53
3q	1.0	2.0	1.7	23
3r	1.2	2.5	2.0	62
3s	0.61	0.9	2.8	38

[a] PT (prothrombin time) is defined as the concentration of compound required to double the time to clot formation in the PT assay. PT_2 values shown are the mean of duplicate measurements. [b] Ex vivo mouse PT prolonging activity was determined 1 h after oral administration to mice at a dose of 30 mg/kg and expressed as ratios of the PT of the compound in treatment mice with that of the untreated group ($n = 3$).

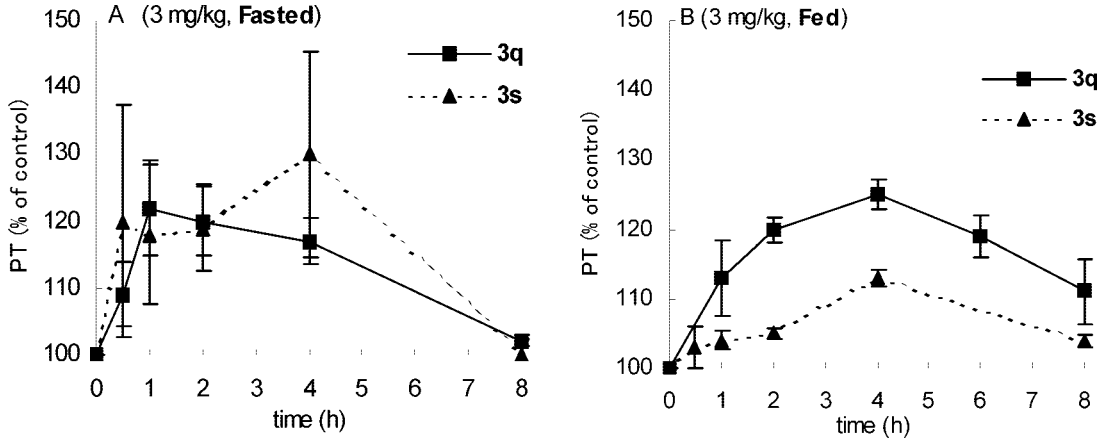

Figure 4. Ex vivo PT prolonging activities of compounds **3q** and **3s** in cynomolgus monkeys ($n = 3$) at 3 mg/kg, po, under fasted conditions (A) and fed conditions (B).

located deeply in the hydrophobic S4 aryl binding site. The S4 pocket is a narrow hydrophobic channel defined by the aromatic rings of Tyr99, Phe174, and Trp215, and hydrophobic interaction with the three aromatic rings in the S4 site has been reported for many potent FXa inhibitors.[24,32c,33] The imidazo[1,5-*c*]imidazol-3-one is sandwiched between the aromatic rings of Tyr99 and that of Phe174 and forms $\pi-\pi$ interactions with the aromatic rings of Tyr99 and Phe174 and a CH−π interaction with the indole ring of Trp215. The carbonyl group of the

Table 7. Selectivity Profile for Compound **3q**

	serine protease				
	FXa	thrombin	trypsin	plasmin	t-PA
K_i (μM)[a]	0.0020 ± 0.0010	6.2 ± 0.4	>60	>60	>60

[a] Data are expressed as the mean ± SEM of three determinations.

Table 8. Pharmacokinetic Parameters for **3q** in Fed Rats and Monkeys[a]

iv (0.3 mg/kg)	rat	monkey
C_{5min} (ng/mL)	291 ± 45	612 ± 98
AUC_{0-24h} (ng·h/mL)	245 ± 38	565 ± 94
MRT (h)	0.7 ± 0.1	1.0 ± 0.2
$V_{d(ss)}$ (mL/kg)	888 ± 149	556 ± 38
CL_{total} (mL/h/kg)	1245 ± 189	541 ± 90

po (3 mg/kg)	rat	monkey
C_{max} (ng/mL)	145 ± 26	269 ± 79
T_{max} (h)	1.2 ± 0.8	2.3 ± 1.5
AUC_{0-24h} (ng·h/mL)	597 ± 159	2592 ± 580
MRT (h)	3.6 ± 0.6	7.0 ± 0.6
BA (%)	24 ± 8	46 ± 6

[a] Data are expressed as the mean ± SD of three determinations.

Table 9. Pharmacokinetic Parameters for **3q** after Oral Administration at a Dose of 3 mg/kg in the Fed and Fasted States[a]

fed state	rat	monkey
C_{max} (ng/mL)	145 ± 26	269 ± 79
T_{max} (h)	1.2 ± 0.8	2.3 ± 1.5
MRT (h)	3.6 ± 0.6	7.0 ± 0.6
AUC_{0-24h} (ng·h/mL)	597 ± 159	2592 ± 580
fasted state	**rat**	**monkey**
C_{max} (ng/mL)	570 ± 90	1204 ± 451
T_{max} (h)	0.3 ± 0.0	0.8 ± 0.3
MRT (h)	1.5 ± 0.4	1.6 ± 0.2
AUC_{0-24h} (ng·h/mL)	417 ± 10	2122 ± 1030

[a] Data are expressed as the mean ± SD of three determinations.

imidazo[1,5-*c*]imidazol-3-one does not appear to interact directly with FXa but rather effects a planarization of the imidazo[1,5-*c*]imidazol-3-one ring and brings it into a perpendicular arrangement with respect to the piperidine ring. The sulfone oxygen is involved in a hydrogen bond with the Gln192 main chain nitrogen.[6d]

Conclusion

In order to address the pharmacokinetic liabilities of our FXa inhibitor **1**, chemical modification of its 4-(imidazo[1,2-*a*]pyridin-5-yl)piperazine moiety to other basic substituents led to the discovery of potent FXa inhibitor 4-(imidazo[1,2-*a*]pyridin-3-yl)piperidine **2** as an interesting new lead. Further modification focused on shifting the imidazole ring into the deeper S4 site and lowering the flexibility and basicity resulting in the discovery of the imidazo[1,5-*c*]imidazol-3-ones **3q**, **3r**, and **3s** as highly potent FXa inhibitors. As a result of further investigation, **3q** showed favorable oral bioavailability in rats and monkeys without significant influence from food intake, good enzyme selectivity, and weak inhibition of CYP3A4. Oral administration of **3q** prevented thrombus formation dose-dependently in rats without a significant increase in bleeding time, unlike warfarin. On the basis of its excellent in vitro and in vivo efficacy and a favorable pharmacokinetic profile, compound **3q** was selected for further evaluation.

Experimental Section

Melting points were determined with a Yanagimoto melting point apparatus or a Büchi melting point apparatus B-545 and are uncorrected. ^{1}H NMR spectra were obtained at 300 or 200 MHz on a Varian Ultra-300 or a Varian Gemini-200 spectrometer. Chemical shifts are given in δ values (ppm) using tetramethylsilane as the internal standard. Reactions were followed by TLC on silica gel 60 F 254 precoated TLC plates (E. Merck) or NH TLC plates (Fuji Silysia Chemical Ltd.). Chromatographic separations were carried out on silica gel 60 (0.063−0.200 or 0.040−0.063 mm, E. Merck) or basic silica gel (ChromatorexNH, 100−200 mesh, Fuji Silysia Chemical Ltd.) using the indicated eluents. Yields are unoptimized. Chemical intermediates were characterized by ^{1}H NMR.

***tert*-Butyl 4-(Imidazo[1,2-*a*]pyridin-3-yl)piperidine-1-carboxylate (6).** A solution of **4** (13.7 g, 44.7 mmol) and **5** (2.63 g, 27.9 mmol) in EtOH (100 mL) was refluxed for 3 h. The reaction mixture was concentrated in vacuo, and the residue was partitioned between EtOAc and water. The aqueous layer was separated, basified with 8 M NaOH to pH 9, and extracted with EtOAc. The extract was washed with brine, dried over anhydrous Na_2SO_4, and concentrated in vacuo. The residue was purified by silica gel chromatography (EtOAc/EtOH = 10/1) to give **6** (8.11 g, 60%) as a pale-yellow solid. ^{1}H NMR (200 MHz, $CDCl_3$) δ: 1.49 (9H, s), 1.59−1.85 (2H, m), 1.98−2.17 (2H, m), 2.83−3.10 (3H, m), 4.18−4.38 (2H, m), 6.83 (1H, t, J = 6.4 Hz), 7.16 (1H, t, J = 8.0 Hz), 7.41 (1H, s), 7.62 (1H, d, J = 9.2 Hz), 7.97 (1H, d, J = 6.8 Hz).

3-(Piperidin-4-yl)imidazo[1,2-*a*]pyridine Dihydrochloride (7a). A solution of **6** (9.04 g, 30.0 mmol) in concentrated HCl (49 mL) was stirred at room temperature for 10 min. The reaction mixture was diluted with EtOH and concentrated in vacuo. The precipitated powder was collected by filtration and washed with EtOH and Et_2O to give **7a** (7.92 g, 91%) as a colorless powder. ^{1}H NMR (200 MHz, D_2O) δ: 1.94−2.22 (2H, m), 2.39−2.59 (2H, m), 3.23−3.48 (2H, m), 3.52−3.78 (3H, m), 7.48−7.61 (1H, m), 7.86 (1H, s), 7.98−8.04 (2H, m), 8.71 (1H, d, J = 7.0 Hz).

3-(Piperidin-4-yl)-5,6,7,8-tetrahydroimidazo[1,2-*a*]pyridine Dihydrochloride (7b). A mixture of **6** (1.51 g, 5.01 mmol) and platinum dioxide (114 mg) in acetic acid (15 mL) was hydrogenated at atmospheric pressure and room temperature for 16 h. The reaction mixture was filtered through a Celite pad, and the filtrate was concentrated in vacuo. The residue was diluted with water, basified with 8 M NaOH to pH 12, and extracted with $CHCl_3$. The extract was washed with brine, dried over anhydrous $MgSO_4$, and concentrated in vacuo to give *tert*-butyl 4-(5,6,7,8-tetrahydroimidazo[1,2-*a*]pyridin-3-yl)piperidine-1-carboxylate (1.53 g, quantitative) as a pale-yellow amorphous powder.

A mixture of *tert*-butyl 4-(5,6,7,8-tetrahydroimidazo[1,2-*a*]pyridin-3-yl)piperidine-1-carboxylate (1.53 g, 5.01 mmol) and concentrated HCl (8.20 mL) was stirred at room temperature for 10 min. The reaction mixture was diluted with 2-propanol and concentrated in vacuo. The precipitate was collected by filtration and washed with 2-propanol and Et_2O to give **7b** (1.32 g, 95%) as a colorless powder. ^{1}H NMR (200 MHz, D_2O) δ: 1.74−2.19 (6H, m), 2.20−2.37 (2H, m), 2.95−3.31 (5H, m), 3.50−3.66 (2H, m), 4.11 (2H, t, J = 5.4 Hz), 7.20 (1H, s).

3-(1-{3-[(6-Chloronaphthalen-2-yl)sulfonyl]propanoyl}piperidin-4-yl)imidazo[1,2-*a*]pyridine Hydrochloride (2). To a solution of **8** (0.74 g, 2.48 mmol) and HOBt (0.57 g, 3.72 mmol) in acetonitrile (15 mL) was added WSC (0.72 g, 3.75 mmol), and the mixture was stirred at room temperature for 15 min. A solution of **7a** (0.82 g, 2.99 mmol), DBU (0.90 mL, 6.02 mmol), and Et_3N (1.05 mL, 7.50 mmol) in acetonitrile (5 mL) was added, and the resulting mixture was stirred at room temperature for 3 h. The reaction mixture was concentrated in vacuo, and the residue was diluted with water and extracted with $CHCl_3$. The extract was washed with brine, dried over anhydrous $MgSO_4$, and concentrated in vacuo. The residue was purified by silica gel chromatography (EtOAc/EtOH = 10/1). To a solution of this product in EtOH (5 mL) was added concentrated HCl (0.38 mL, 4.60 mmol), and the resulting mixture was concentrated in vacuo. The residue was diluted with EtOH and Et_2O, and the precipitate was collected by filtration to give **2** (1.14 g, 81%) as a colorless powder, mp 224−225 °C. ^{1}H NMR (300 MHz, DMSO-d_6) δ: 1.28−1.39 (1H, m), 1.39−1.68 (1H, m), 1.93−2.11 (2H, m), 2.62−2.84 (3H, m), 3.12−3.28 (1H, m), 3.32−3.57 (1H, m), 3.61−3.72 (2H, m), 3.88−4.01 (1H, m), 4.31−4.45 (1H, m), 7.54 (1H, t, J = 6.6 Hz), 7.73 (1H, dd, J = 7.4 and 6.0 Hz), 7.93−8.04 (4H, m), 8.19 (1H, d, J = 8.7 Hz), 8.26−8.31 (2H, m), 8.68 (1H, s), 9.02 (1H, d, J = 6.9 Hz). Anal. ($C_{25}H_{24}ClN_3O_3S\cdot HCl\cdot H_2O$) C, H, N.

3-(1-{3-[(6-Chloronaphthalen-2-yl)sulfonyl]propanoyl}piperidin-4-yl)-5,6,7,8-tetrahydroimidazo[1,2-*a*]pyridine Hydrochloride (3a). Compound **3a** was prepared in a manner similar to that described for **2** in 82% yield as a colorless powder, mp 213−214 °C. ^{1}H NMR (200 MHz, DMSO-d_6) δ: 1.12−1.58 (2H, m), 1.76−2.08 (6H, m), 2.48−2.68 (2H, m), 2.75 (2H, t, J = 7.4 Hz), 2.84−3.19 (3H, m), 3.64 (2H, t, J = 7.0 Hz), 3.34−3.99 (1H, m), 4.00−4.12 (2H, m), 4.26−4.40 (1H, m), 7.34 (1H, s), 7.74 (1H, dd, J = 8.8 and 2.2 Hz), 8.01 (1H, dd, J = 8.8 and 1.8 Hz), 8.17−8.32 (3H, m), 8.67 (1H, s). Anal. ($C_{25}H_{28}ClN_3O_3S\cdot HCl\cdot H_2O$) C, H, N.

1-{3-[(6-Chloronaphthalen-2-yl)sulfonyl]propanoyl}-4-(1*H*-imidazol-4-yl)piperidine (3b). To a mixture of **8** (0.60 g, 2.00 mmol) and HOBt (0.46 g, 3.00 mmol) in acetonitrile (15 mL) was added WSC (0.58 g, 3.00 mmol), and the mixture was stirred at room temperature for 15 min. A solution of **9a** (0.46 g, 2.00 mmol),

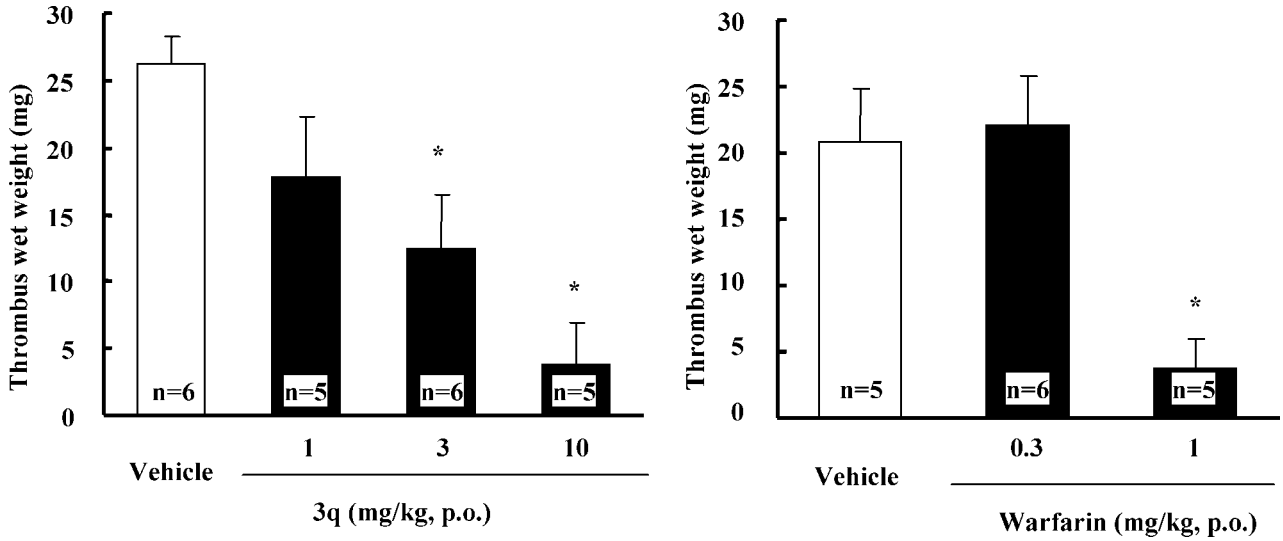

Figure 5. Antithrombotic effect of **3q** and warfarin in a rat venous thrombosis model. Thrombus formation was stimulated by the combination of endothelial damage and blood stagnation. Data are expressed as the mean ± SEM: (*) $p = 0.025$ vs vehicle (a one-tailed Williams test), $n = 5-6$.

Table 10. Effect of **3q** and Warfarin on Bleeding Time in Rats[a]

	dose (mg/kg, po)	bleeding time (s)
vehicle		460 ± 60
3q	30	490 ± 90
	100	1040 ± 296
vehicle		360 ± 35
warfarin	0.3	445 ± 87
	1	1590 ± 158[b]

[a] Data are expressed as the mean ± SEM. [b] $p \leq 0.025$ vs vehicle (a one-tailed Shirley−Williams' test). $n = 6$.

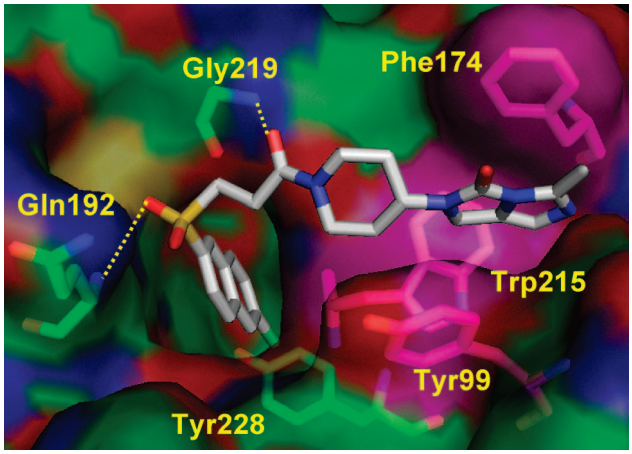

Figure 6. Binding model of imidazo[1,5-*c*]imidazol-3-one **3q** in FXa.

DBU (0.61 g, 4.00 mmol), and Et_3N (0.61 g, 6.00 mmol) in acetonitrile (15 mL) was added to the mixture, and the resulting mixture was stirred at room temperature for 15 h. The reaction mixture was concentrated in vacuo, and the residue was diluted with aqueous K_2CO_3 solution and extracted with EtOAc. The extract was washed with brine, dried over anhydrous Na_2SO_4, and concentrated in vacuo. The residue was purified by basic silica gel chromatography (EtOAc) to give **3b** (0.43 g, 50%) as a colorless amorphous powder. ^{1}H NMR (300 MHz, $CDCl_3$ + CD_3OD) δ: 1.40−1.60 (2H, m), 1.95−2.11 (2H, m), 2.66−2.91 (5H, m), 3.13−3.20 (1H, m), 3.54−3.61 (2H, m), 3.86−3.90 (1H, m), 4.47−4.51 (1H, m), 6.70 (1H, s), 7.53 (1H, d, $J = 1.2$ Hz), 7.59 (1H, dd, $J = 8.4$ and 2.4 Hz), 7.93−7.98 (4H, m), 8.48 (1H, s). Anal. ($C_{21}H_{22}ClN_3O_3 \cdot 0.5H_2O$) C, H, N.

1-{3-[(6-Chloronaphthalen-2-yl)sulfonyl]propanoyl}-4-(2-methyl-1*H*-imidazol-4-yl)piperidine (3c). Compound **3c** was prepared in a manner similar to that described for **3b** in 91% yield as a colorless powder, mp 190−192 °C. ^{1}H NMR (200 MHz, $CDCl_3$) δ: 1.41−1.60 (2H, m), 1.93−2.10 (2H, m), 2.39 (3H, s), 2.59−2.71 (2H, m), 2.83−2.91 (2H, m), 3.07−3.21 (1H, m), 3.53−3.60 (2H, m), 3.83−3.90 (1H, m), 4.47−4.54 (1H, m), 6.56 (1H, s), 7.58 (1H, dd, $J = 9.0$ and 2.0 Hz), 7.88−7.97 (4H, m), 8.48 (1H, br s). Anal. ($C_{22}H_{24}ClN_3O_3S \cdot 0.2H_2O$) C, H, N.

1-{3-[(6-Chloronaphthalen-2-yl)sulfonyl]propanoyl}-4-(1-trityl-1*H*-imidazol-4-yl)piperidine (10a). To a solution of **3b** (0.35 g, 0.81 mmol) and Et_3N (0.10 g, 1.00 mmol) in DMF (10 mL) was added trityl chloride (0.25 g, 0.90 mmol) at 0 °C, and the resulting mixture was stirred at 0 °C for 1 h and then at room temperature for 15 h. The reaction mixture was concentrated in vacuo, and the residue was diluted with saturated aqueous $NaHCO_3$ solution and extracted with EtOAc. The extract was washed with brine, dried over anhydrous Na_2SO_4, and concentrated in vacuo. The residue was purified by basic silica gel chromatography (EtOAc) to give **10a** (0.54 g, quantitative) as a colorless amorphous powder. ^{1}H NMR (200 MHz, $CDCl_3$) δ: 1.40−1.50 (2H, m), 1.92−2.10 (2H, m), 2.58−2.87 (4H, m), 3.04−3.17 (1H, m), 3.51−3.59 (2H, m), 3.78−3.84 (1H, m), 4.41−4.47 (1H, m), 6.49 (1H, s), 7.09−7.35 (16H, m), 7.57 (1H, dd, $J = 8.8$ and 1.8 Hz), 7.92−8.02 (4H, m), 8.46 (1H, s).

1-{3-[(6-Chloronaphthalen-2-yl)sulfonyl]propanoyl}-4-(2-methyl-1-trityl-1*H*-imidazol-4-yl)piperidine (10b). Compound **10b** was prepared in a manner similar to that described for **10a** in 60% yield as a colorless amorphous powder. ^{1}H NMR (300 MHz, $CDCl_3$) δ: 1.33−1.59 (2H, m), 1.90−2.06 (2H, m), 2.57−2.74 (2H, m), 2.82−2.89 (2H, m), 3.05−3.13 (1H, m), 3.52−3.57 (2H, m), 3.80−3.84 (1H, m), 4.45−4.49 (1H, m), 6.34 (1H, s), 7.09−7.12 (5H, m), 7.30−7.35 (10H, m), 7.58 (1H, dd, $J = 8.7$ and 1.8 Hz), 7.91−7.96 (4H, m), 8.47 (1H, s).

1-{3-[(6-Chloronaphthalen-2-yl)sulfonyl]propanoyl}-4-(1-methyl-1*H*-imidazol-5-yl)piperidine (3d). A solution of **10a** (0.54 g, 0.80 mmol) and iodomethane (0.10 mL, 1.61 mmol) in DMF (5 mL) was stirred at room temperature for 15 h. The reaction mixture was concentrated in vacuo, and the residue was dissolved in acetic acid (5 mL), water (5 mL), and MeOH (2 mL). After being stirred at 95 °C for 2 h, the reaction mixture was concentrated in vacuo. The residue was basified with saturated aqueous $NaHCO_3$ solution and extracted with EtOAc. The extract was washed with saturated aqueous $NaHCO_3$ solution, dried over anhydrous Na_2SO_4, and concentrated in vacuo. The residue was purified by basic silica gel chromatography (EtOAc to 10/1 EtOAc/MeOH) to give **3d** (0.27

g, 76%) as a colorless amorphous powder. ^{1}H NMR (200 MHz, $CDCl_3$) δ: 1.43−1.70 (2H, m), 1.88−2.04 (2H, m), 2.60−2.78 (2H, m), 2.87−2.95 (2H, m), 3.09−3.22 (1H, m), 3.53−3.61 (2H, m), 3.60 (3H, s), 3.91−3.98 (1H, m), 4.55−4.62 (1H, m), 6.76 (1H, s), 7.38 (1H, s), 7.59 (1H, dd, J = 8.8 and 1.8 Hz), 7.93−7.97 (4H, m), 8.48 (1H, s). Anal. ($C_{22}H_{24}ClN_3O_3S\cdot0.5H_2O$) C, H, N.

1-{3-[(6-Chloronaphthalen-2-yl)sulfonyl]propanoyl}-4-(1,2-dimethyl-1*H*-imidazol-5-yl)piperidine (3e). Compound **3e** was prepared in a manner similar to that described for **3d** in 48% yield as a colorless amorphous powder. ^{1}H NMR (200 MHz, $CDCl_3$) δ: 1.40−1.56 (2H, m), 1.87−2.00 (2H, m), 2.36 (3H, s), 2.60−2.71 (2H, m), 2.87−2.95 (2H, m), 3.09−3.21 (1H, m), 3.45 (3H, s), 3.53−3.61 (2H, m), 3.90−3.96 (1H, m), 4.54−4.60 (1H, m), 6.60 (1H, s), 7.60 (1H, dd, J = 8.8 and 1.8 Hz), 7.93−7.97 (4H, m), 8.49 (1H, s). Anal. ($C_{23}H_{26}ClN_3O_3S\cdot H_2O$) C, H, N.

***tert*-Butyl 4-(2-Ethyl-1*H*-imidazol-1-yl)piperidine-1-carboxylate (13a).** A mixture of **11** (10.0 g, 35.8 mmol), **12a** (4.13 g, 43.0 mmol), and K_2CO_3 (4.95 g, 35.8 mmol) in DMF (80 mL) was stirred at 100 °C for 72 h. The reaction mixture was concentrated in vacuo, and the residue was diluted with aqueous $NaHCO_3$ solution and extracted with EtOAc. The extract was washed with saturated aqueous $NaHCO_3$ solution, dried over anhydrous Na_2SO_4, and concentrated in vacuo. The residue was purified by basic silica gel chromatography (EtOAc to 5/1 EtOAc/MeOH) to give **13a** (1.10 g, 11%) as a yellow oil. ^{1}H NMR (300 MHz, $CDCl_3$) δ: 1.31−1.39 (3H, m), 1.49 (9H, s), 1.70−1.95 (4H, m), 2.67−2.87 (4H, m), 3.96−4.01 (1H, m), 4.29−4.33 (2H, m), 6.86 (1H, d, J = 1.5 Hz), 6.97 (1H, d, J = 1.5 Hz).

***tert*-Butyl 4-(2-Propyl-1*H*-imidazol-1-yl)piperidine-1-carboxylate (13b).** Compound **13b** was prepared in a manner similar to that described for **13a** in 3% yield as a colorless amorphous powder. ^{1}H NMR (300 MHz, $CDCl_3$) δ: 0.98−1.04 (3H, m), 1.49 (9H, s), 1.71−1.94 (6H, m), 2.59−2.69 (2H, m), 2.79−2.87 (2H, m), 3.96−4.04 (1H, m), 4.28−4.33 (2H, m), 6.85 (1H, d, J = 1.2 Hz), 6.97 (1H, d, J = 1.5 Hz).

1-{3-[(6-Chloronaphthalen-2-yl)sulfonyl]propanoyl}-4-(1*H*-imidazol-1-yl)piperidine (3h). A mixture of **13c** (0.28 g, 1.11 mmol) in concentrated HCl (4 mL) was stirred at room temperature for 3 h. The reaction mixture was concentrated in vacuo, and the residue was azeotroped with EtOH. The residue, DBU (0.33 mL, 2.23 mmol), and Et_3N (0.47 mL, 3.36 mmol) were dissolved in acetonitrile (15 mL). The solution was added to a mixture of **8** (0.33 g, 1.10 mmol), HOBt (0.26 g, 1.70 mmol), and WSC (0.32 g, 1.70 mmol) in acetonitrile (15 mL), and the resulting mixture was stirred at room temperature for 15 h. The reaction mixture was concentrated in vacuo, and the residue was diluted with aqueous K_2CO_3 solution and extracted with EtOAc. The extract was dried over anhydrous Na_2SO_4 and concentrated in vacuo. The residue was purified by basic silica gel chromatography (EtOAc) to give **3h** (0.40 g, 83%) as a yellow gum. ^{1}H NMR (300 MHz, $CDCl_3$) δ: 1.70−1.92 (2H, m), 2.09−2.22 (2H, m), 2.64−2.72 (1H, m), 2.90−2.97 (2H, m), 3.17−3.25 (1H, m), 3.54−3.61 (2H, m), 4.00−4.09 (1H, m), 4.08−4.21 (1H, m), 4.69−4.73 (1H, m), 6.93 (1H, t, J = 1.2 Hz), 7.08 (1H, d, J = 1.2 Hz), 7.54 (1H, s), 7.60 (1H, dd, J = 8.7 and 2.1 Hz), 7.93−7.97 (4H, m), 8.49 (1H, d, J = 1.2 Hz). Anal. ($C_{21}H_{22}ClN_3O_3S\cdot0.5H_2O$) C, H, N.

The following compounds **3f**, **3g**, and **3i** were prepared in a manner similar to that described for **3h**.

1-{3-[(6-Chloronaphthalen-2-yl)sulfonyl]propanoyl}-4-(2-ethyl-1*H*-imidazol-1-yl)piperidine (3f). Yield 98%, colorless amorphous powder. ^{1}H NMR (300 MHz, $CDCl_3$) δ: 1.36 (3H, t, J = 7.4 Hz), 1.65−1.86 (2H, m), 1.96−2.05 (2H, m), 2.61−2.68 (1H, m), 2.71 (2H, q, J = 7.5 Hz), 2.91−2.98 (2H, m), 3.16−3.24 (1H, m), 3.54−3.62 (2H, m), 4.01−4.13 (2H, m), 4.73−4.77 (1H, m), 6.81 (1H, d, J = 1.8 Hz), 6.98 (1H, d, J = 1.5 Hz), 7.60 (1H, dd, J = 8.7 and 1.8 Hz), 7.94−7.97 (4H, m), 8.49 (1H, d, J = 0.6 Hz). Anal. ($C_{23}H_{26}ClN_3O_3S\cdot0.5H_2O$) C, H, N.

1-{3-[(6-Chloronaphthalen-2-yl)sulfonyl]propanoyl}-4-(2-propyl-1*H*-imidazol-1-yl)piperidine (3g). Yield 66%, colorless amorphous powder. ^{1}H NMR (200 MHz, $CDCl_3$) δ: 1.02 (3H, t, J = 7.5 Hz), 1.68−2.05 (6H, m), 2.62−2.69 (3H, m), 2.90−2.99 (2H, m), 3.14−3.26 (1H, m), 3.54−3.63 (2H, m), 4.01−4.14 (2H, m), 4.71−4.78 (1H, m), 6.80 (1H, d, J = 1.4 Hz), 6.97 (1H, d, J = 1.0 Hz), 7.60 (1H, dd, J = 8.8 and 1.8 Hz), 7.89−7.98 (4H, m), 8.49 (1H, s). Anal. ($C_{24}H_{28}ClN_3O_3S\cdot0.5H_2O$) C, H, N.

1-{3-[(6-Chloronaphthalen-2-yl)sulfonyl]propanoyl}-4-(2-methyl-1*H*-imidazol-1-yl)piperidine (3i). Yield 83%, colorless amorphous powder. ^{1}H NMR (300 MHz, $CDCl_3$) δ: 1.68−1.84 (2H, m), 1.97−2.09 (2H, m), 2.42 (3H, s), 2.61−2.69 (1H, m), 2.91−2.98 (2H, m), 3.15−3.24 (1H, m), 3.54−3.62 (2H, m), 4.02−4.13 (2H, m), 4.73−4.77 (1H, m), 6.81 (1H, d, J = 1.5 Hz), 6.94 (1H, d, J = 1.5 Hz), 7.60 (1H, dd, J = 8.9 and 2.0 Hz), 7.91−7.97 (4H, m), 8.50 (1H, s). Anal. ($C_{22}H_{24}ClN_3O_3S\cdot H_2O$) C, H, N.

***tert*-Butyl 4-(1-Methyl-1*H*-imidazol-2-yl)piperidine-1-carboxylate (15).** To a solution of **14** (0.25 g, 1.00 mmol) in DMF (3 mL) was added NaH (60% in oil, 40 mg, 1.00 mmol) at 0 °C, and the mixture was stirred at 0 °C for 30 min. Iodomethane (0.07 mL, 1.12 mmol) was added to the mixture, and then the resulting mixture was stirred at 0 °C for 2 h. The reaction mixture was concentrated in vacuo, and the residue was diluted with aqueous $NaHCO_3$ solution and extracted with EtOAc. The extract was dried over anhydrous Na_2SO_4 and concentrated in vacuo. The residue was purified by silica gel chromatography ($CHCl_3$/MeOH = 10/1) to give **15** (0.27 g, quantitative) as a pale-yellow oil. ^{1}H NMR (200 MHz, $CDCl_3$) δ: 1.46 (9H, s), 1.80−1.91 (4H, m), 2.70−2.96 (3H, m), 3.61 (3H, s), 4.18−4.25 (2H, m), 6.79 (1H, d, J = 1.0 Hz), 6.94 (1H, d, J = 1.0 Hz).

1-{3-[(6-Chloronaphthalen-2-yl)sulfonyl]propanoyl}-4-(1*H*-imidazol-2-yl)piperidine (3j). Compound **3j** was prepared in a manner similar to that described for **3h** in 54% yield as a colorless amorphous powder. ^{1}H NMR (300 MHz, $CDCl_3$) δ: 1.60−1.85 (2H, m), 1.98−2.14 (2H, m), 2.72−3.04 (4H, m), 3.15−3.24 (1H, m), 3.49−3.61 (2H, m), 3.90−3.95 (1H, m), 4.46−4.50 (1H, m), 6.96 (1H, br s), 7.00 (1H, br s), 7.58 (1H, dd, J = 2.1 and 9.0 Hz), 7.90−7.97 (4H, m), 8.48 (1H, d, J = 0.9 Hz), 8.88 (1H, br s). Anal. ($C_{21}H_{22}ClN_3O_3S$) C, H, N.

1-{3-[(6-Chloronaphthalen-2-yl)sulfonyl]propanoyl}-4-(1-methyl-1*H*-imidazol-2-yl)piperidine (3k). Compound **3k** was prepared in a manner similar to that described for **3h** in 70% yield as a colorless amorphous powder. ^{1}H NMR (200 MHz, $CDCl_3$) δ: 1.60−2.00 (4H, m), 2.70−2.94 (4H, m), 3.11−3.26 (1H, m), 3.52−3.61 (2H, m), 3.61 (3H, s), 3.93−4.00 (1H, m), 4.45−4.52 (1H, m), 6.79 (1H, d, J = 1.2 Hz), 6.92 (1H, d, J = 1.4 Hz), 7.58 (1H, dd, J = 2.0 and 8.8 Hz), 7.89−7.98 (4H, m), 8.48 (1H, s), 8.88 (1H, br s). Anal. ($C_{22}H_{24}ClN_3O_3S\cdot0.5H_2O$) C, H, N.

***tert*-Butyl 4-[(2-Methyl-1*H*-imidazol-1-yl)methyl]piperidine-1-carboxylate (17a).** To a solution of **16a** (8.50 g, 30.6 mmol) and 2-methylimidazole (1.80 g, 21.9 mmol) in DMF (100 mL) was added NaH (60% in oil, 0.87 g, 21.8 mmol) at room temperature. After the mixture was stirred at 80 °C for 12 h, the reaction mixture was concentrated in vacuo. The residue was diluted with $CHCl_3$, washed with aqueous K_2CO_3 solution, dried over anhydrous Na_2SO_4, and concentrated in vacuo. The residue was purified by silica gel chromatography (EtOAc to 5/1 EtOAc/MeOH) to give **17a** (0.43 g, 7%) as a brown oil. ^{1}H NMR (300 MHz, $CDCl_3$) δ: 1.13−1.26 (2H, m), 1.46 (9H, s), 1.68 (1H, m), 2.37 (3H, s), 2.67 (2H, t, J = 11.4 Hz), 3.86 (2H, t, J = 7.5 Hz), 4.11 (2H, br s), 6.80 (1H, d, J = 1.5 Hz), 6.91 (1H, d, J = 1.5 Hz).

The following compounds **17b−d** were prepared in a manner similar to that described for **17a**.

***tert*-Butyl 4-[2-(2-Methyl-1*H*-imidazol-1-yl)ethyl]piperidine-1-carboxylate (17b).** Yield 80%, brown oil. ^{1}H NMR (300 MHz, $CDCl_3$) δ: 1.13−1.28 (2H, m), 1.46 (9H, s), 1.57−1.63 (4H, m), 1.82 (1H, m), 2.37 (3H, s), 2.65 (2H, t, J = 12.9 Hz), 3.71 (2H, d, J = 7.5 Hz), 4.16 (2H, br s), 6.78 (1H, d, J = 1.5 Hz), 6.91 (1H, d, J = 1.5 Hz).

***tert*-Butyl 4-[3-(2-Methyl-1*H*-imidazol-1-yl)propyl]piperidine-1-carboxylate (17c).** Yield quantitative, brown oil. ^{1}H NMR (300 MHz, $CDCl_3$) δ: 1.03−1.35 (4H, m), 1.45 (9H, s), 1.59−1.82 (5H, m), 2.37 (3H, s), 2.66 (2H, t, J = 12.4 Hz), 3.81 (2H, t, J = 7.0 Hz), 4.06 (2H, br s), 6.80 (1H, d, J = 1.4 Hz), 6.90 (1H, d, J = 1.4 Hz).

***tert*-Butyl 4-[4-(2-Methyl-1*H*-imidazol-1-yl)butyl]piperidine-1-carboxylate (17d).** Yield 47%, brown oil. ^{1}H NMR (300 MHz, $CDCl_3$) δ: 1.03−1.35 (4H, m), 1.45 (9H, s), 1.59−1.82 (7H, m), 2.37 (3H, s), 2.66 (2H, t, J = 12.4 Hz), 3.81 (2H, t, J = 7.0 Hz), 4.06 (2H, br s), 6.80 (1H, d, J = 1.4 Hz), 6.90 (1H, d, J = 1.4 Hz).

1-{3-[(6-Chloronaphthalen-2-yl)sulfonyl]propanoyl}-4-[(2-methyl-1*H*-imidazol-1-yl)methyl]piperidine Hydrochloride (3l). **17a** (0.43 g, 1.54 mmol) was dissolved in concentrated HCl (4 mL) and diluted with EtOH (20 mL). The solution was concentrated in vacuo, and the residue was dissolved in acetonitrile (20 mL) with Et_3N (0.63 mL, 4.51 mmol) and DBU (0.46 mL, 3.26 mmol). The solution was added to a mixture of **8** (0.45 g, 1.50 mmol), WSC (0.43 g, 2.24 mmol), and HOBt (0.35 g, 2.29 mmol) in acetonitrile (10 mL), and then the resulting mixture was stirred at room temperature for 12 h. The reaction mixture was concentrated in vacuo, diluted with saturated aqueous $NaHCO_3$ solution, and extracted with $CHCl_3$. The extract was dried over anhydrous Na_2SO_4 and concentrated in vacuo. The residue was purified by silica gel chromatography (EtOAc), and the product was dissolved in EtOAc. An amount of 4 M HCl in EtOAc (0.30 mL, 1.20 mmol) was added, and then the mixture was stirred at room temperature for 5 min. The resulting mixture was concentrated in vacuo, and the residue was triturated with Et_2O to give **3l** (0.55 g, 74%) as a beige amorphous powder. ^{1}H NMR (200 MHz, DMSO-d_6) δ: 1.04−1.25 (2H, m), 1.63−1.73 (2H, m), 1.91 (1H, m), 2.37 (3H, s), 2.52 (1H, m), 2.82−3.04 (3H, m), 3.51−3.60 (2H, m), 3.70 (2H, d, J = 7.4 Hz), 3.88 (1H, d, J = 13.4 Hz), 4.56 (1H, d, J = 13.4 Hz), 6.76 (1H, d, J = 1.4 Hz), 6.92 (1H, d, J = 1.4 Hz), 7.60 (1H, dd, J = 2.0 and 8.8 Hz), 7.87−7.97 (4H, m), 8.48 (1H, s). Anal. ($C_{23}H_{26}ClN_3O_3S\cdot HCl\cdot H_2O\cdot 0.25Et_2O$) C, H, N.

The following compounds **3m** and **3n** were prepared in a manner similar to that described for **3l**.

1-{3-[(6-Chloronaphthalen-2-yl)sulfonyl]propanoyl}-4-[2-(2-methyl-1*H*-imidazol-1-yl)ethyl]piperidine Hydrochloride (3m). Yield 69%, beige amorphous powder. ^{1}H NMR (200 MHz, DMSO-d_6) δ: 1.00−1.24 (2H, m), 1.48 (1H, m), 1.63−1.77 (4H, m), 2.37 (3H, s), 2.49 (1H, t, J = 13.2 Hz), 2.83−2.90 (2H, m), 2.98 (1H, t, J = 13.2 Hz), 3.47−3.60 (2H, m), 3.80−3.88 (3H, m), 4.49 (1H, d, J = 11.4 Hz), 6.79 (1H, s), 6.91 (1H, s), 7.59 (1H, dd, J = 1.8 and 9.0 Hz), 7.90−7.96 (4H, m), 8.47 (1H, s). Anal. ($C_{24}H_{28}ClN_3O_3S\cdot HCl\cdot 0.25H_2O$) C, H, N.

1-{3-[(6-Chloronaphthalen-2-yl)sulfonyl]propanoyl}-4-[3-(2-methyl-1*H*-imidazol-1-yl)propyl]piperidine Hydrochloride (3n). Yield 53%, beige amorphous powder. ^{1}H NMR (200 MHz, $CDCl_3$) δ: 1.00−1.31 (4H, m), 1.52 (1H, m), 1.65−1.88 (4H, m), 2.37 (3H, s), 2.49 (1H, t, J = 11.1 Hz), 2.83−2.90 (2H, m), 3.00 (1H, t, J = 11.1 Hz), 3.47−3.58 (2H, m), 3.84 (1H, d, J = 14.1 Hz), 4.02 (2H, t, J = 6.9 Hz), 4.51 (1H, d, J = 14.1 Hz), 7.05 (1H, s), 7.05 (1H, s), 7.28 (1H, s), 7.61 (1H, dd, J = 2.1 and 9.0 Hz), 7.89−7.97 (4H, m), 8.47 (1H, s). Anal. ($C_{25}H_{30}ClN_3O_3S\cdot HCl\cdot H_2O$) C, H, N.

1-{3-[(6-Chloronaphthalen-2-yl)sulfonyl]propanoyl}-4-[4-(2-methyl-1*H*-imidazol-1-yl)butyl]piperidine (3o). Compound **3o** was prepared in a manner similar to that described for **3h** in 15% yield as a beige amorphous powder. ^{1}H NMR (200 MHz, $CDCl_3$) δ: 0.91−1.08 (2H, m), 1.22−1.43 (5H, m), 1.61−1.74 (4H, m), 2.37 (3H, s), 2.40−2.54 (1H, m), 2.81 −3.02 (3H, m), 3.52−3.60 (2H, m), 3.78−3.85 (3H, m), 4.26 (1H, d, J = 13.2 Hz), 6.79 (1H, d, J = 1.4 Hz), 6.90 (1H, d, J = 1.4 Hz), 7.58 (1H, dd, J = 2.0 and 8.8 Hz), 7.92−7.97 (4H, m), 8.47 (1H, s). Anal. ($C_{26}H_{32}ClN_3O_3S\cdot 0.5H_2O$) C, H, N.

***tert*-Butyl 4-[(2-Methyl-1*H*-imidazol-1-yl)acetyl]piperazine-1-carboxylate (19).** To a solution of 2-methylimidazole (1.10 g, 13.3 mmol) in DMF was added NaH (60% in oil, 0.62 g, 15.5 mmol) at 0 °C. After the mixture was stirred at 0 °C for 30 min, **18** (4.09 g, 13.3 mmol) was added to the mixture, and then the resulting mixture was stirred at 50 °C for 1 h. The reaction mixture was concentrated in vacuo, diluted with aqueous K_2CO_3 solution, and extracted with EtOAc. The extract was dried over anhydrous Na_2SO_4 and concentrated in vacuo to give **19** (2.80 g, 68%) as a colorless oil. ^{1}H NMR (200 MHz, $CDCl_3$) δ: 1.48 (9H, s), 2.33 (3H, s), 3.44−3.50 (6H, m), 3.60−3.71 (2H, m), 4.67 (2H, s), 6.80 (1H, d, J = 1.6 Hz), 6.94 (1H, d, J = 1.6 Hz).

1-[2-(2-Methyl-1*H*-imidazole-1-yl)ethyl]piperazine (20). 19 (2.80 g, 9.08 mmol) was dissolved in TFA (15 mL), and the resulting mixture was stirred at room temperature for 1 h. The reaction mixture was concentrated in vacuo, diluted with saturated aqueous $NaHCO_3$ solution, and extracted with $CHCl_3$. The extract was dried over anhydrous Na_2SO_4 and concentrated in vacuo. The residue was dissolved in THF (30 mL), and lithium aluminum hydride (0.46 g, 12.1 mmol) was added to the solution at 0 °C. After being stirred at 60 °C for 1 h, the reaction mixture was cooled to 0 °C. The reaction mixture was quenched with saturated ammonium chloride and extracted with EtOAc. The extract was dried over anhydrous Na_2SO_4 and concentrated in vacuo to give **20** (0.70 g, 40%) as a colorless oil. ^{1}H NMR (200 MHz, DMSO-d_6) δ: 2.27 (3H, s), 2.49−2.69 (8H, m), 3.60 (2H, t, J = 9.1 Hz), 3.89 (2H, t, J = 9.1 Hz), 6.69 (1H, d, J = 1.6 Hz), 7.02 (1H, d, J = 1.6 Hz).

1-{3-[(6-Chloronaphthalen-2-yl)sulfonyl]propanoyl}-4-[2-(2-methyl-1*H*-imidazol-1-yl)ethyl]piperazine (3p). To a solution of **8** (0.90 g, 3.01 mmol), **20** (0.58 g, 3.01 mmol), Et_3N (1.26 mL, 9.03 mmol), and HOBt (0.69 g, 4.52 mmol) in CH_2Cl_2 (30 mL) was added WSC (0.87 g, 4.52 mmol) at room temperature. After being stirred at room temperature for 16 h, the reaction mixture was concentrated in vacuo, diluted with saturated aqueous $NaHCO_3$ solution, and extracted with $CHCl_3$. The extract was dried over anhydrous Na_2SO_4 and concentrated in vacuo. The residue was purified by silica gel chromatography ($CHCl_3$/MeOH = 40/1 to 10/1) to give **3p** (0.021 g, 2%) as a brown amorphous powder. ^{1}H NMR (200 MHz, $CDCl_3$) δ: 2.39 (3H, s), 2.41−2.46 (4H, m), 2.61−2.67 (2H, m), 2.82−2.89 (2H, m), 3.42−3.60 (6H, m), 3.93 (2H, t, J = 9.3 Hz), 6.85 (1H, d, J = 2.1 Hz), 6.90 (1H, d, J = 2.1 Hz), 7.59 (1H, dd, J = 2.4 and 13.2 Hz), 7.92−7.94 (4H, m), 8.47 (1H, s). Anal. ($C_{23}H_{27}ClN_4O_3S\cdot H_2O$) C, H, N.

***tert*-Butyl4-{[(2-Methyl-1*H*-imidazol-5-yl)methyl]amino}piperidine-1-carboxylate (23a).** A mixture of **21** (2.00 g, 10.0 mmol), **22a** (1.10 g, 10.0 mmol), acetic acid (0.69 mL, 12.0 mmol), and sodium triacetoxyborohydride (5.30 g, 25.0 mmol) in MeOH (40 mL) was stirred at room temperature for 2 h. The reaction mixture was concentrated in vacuo, and the residue was basified with aqueous K_2CO_3 solution. The solution was extracted with EtOAc, and the extract was dried over anhydrous Na_2SO_4 and concentrated in vacuo to give **23a** (2.94 g, quantitative) as a pale-yellow oil. ^{1}H NMR (300 MHz, $CDCl_3$) δ: 1.26 (2H, t, J = 7.2 Hz), 1.45 (9H, s), 1.86 (2H, d, J = 12.6 Hz), 2.40 (3H, s), 2.61−2.86 (3H, m), 3.74 (2H, s), 3.86−4.18 (2H, m), 6.75 (1H, s).

***tert*-Butyl 4-{[(2,4-Dimethyl-1*H*-imidazol-5-yl)methyl]amino}piperidine-1-carboxylate (23b).** Compound **23b** was prepared in a manner similar to that described for **23a** in quantitative yield as a pale-yellow oil. ^{1}H NMR (300 MHz, $CDCl_3$) δ: 1.28−1.40 (2H, m), 1.45 (9H, s), 1.87 (2H, d, J = 12.3 Hz), 2.14 (3H, s), 2.33 (3H, s), 2.67−2.80 (3H, m), 3.71 (2H, s), 4.06 (2H, br s), 6.06 (1H, s).

***tert*-Butyl 4-(5-Methyl-3-oxo-1*H*-imidazo[1,5-*c*]imidazol-2(3*H*)-yl)piperidine-1-carboxylate (24a).** To a solution of compound **23a** (2.94 g, 10.0 mmol) in acetonitrile (20 mL) was added DBU (1.50 mL, 10.0 mmol) and CDI (1.62 g, 10.0 mmol), and the mixture was stirred at room temperature for 15 h. The reaction mixture was concentrated in vacuo, diluted with aqueous K_2CO_3 solution, and extracted with EtOAc. The extract was dried over anhydrous $MgSO_4$ and concentrated in vacuo. The residue was purified by silica gel chromatography (EtOAc to 10/1 EtOAc/MeOH) to give **24a** (2.45 g, 77%) as a pale-yellow solid. ^{1}H NMR (300 MHz, $CDCl_3$) δ: 1.47 (9H, s), 1.63−1.73 (2H, m), 1.75−1.98 (2H, m), 2.61 (3H, s), 2.83 (2H, t, J = 12.7 Hz), 4.10 (1H, tt, J = 12.1 and 4.1 Hz), 4.28 (4H, s), 6.71 (1H, t, J = 1.5 Hz).

***tert*-Butyl 4-(5,7-Dimethyl-3-oxo-1*H*-imidazo[1,5-*c*]imidazol-2(3*H*)-yl)piperidine-1-carboxylate (24b).** Compound **24b** was prepared in a manner similar to that described for **24a** in 97% yield as a pale-yellow oil. ^{1}H NMR (200 MHz, $CDCl_3$) δ: 1.47 (9H, s), 1.57−1.72 (2H, m), 1.79−1.84 (2H, m), 2.15 (3H, s), 2.57 (3H,

s), 2.82 (2H, t, J = 12.7 Hz), 4.03−4.15 (1H, m), 4.20 (2H, s), 4.29 (1H, br s).

2-(1-{3-[(6-Chloronaphthalen-2-yl)sulfonyl]propanoyl}piperidin-4-yl)-5-methyl-1,2-dihydro-3*H*-imidazo[1,5-*c*]imidazol-3-one (3q). 24a (1.18 g, 3.69 mmol) was dissolved in concentrated HCl (4 mL), and the resulting mixture was stirred at room temperature for 30 min. The reaction mixture was concentrated in vacuo. The residual solid, **8** (1.00 g, 3.35 mmol), HOBt (0.62 g, 4.02 mmol), and Et_3N (1.68 mL, 12.1 mmol) were suspended in DMF (7 mL). WSC (0.77 g, 4.02 mmol) was added to the suspension, and then the resulting mixture was stirred at room temperature for 5 h. The reaction mixture was cooled to 0 °C and diluted with water (14 mL). After the mixture was stirred at 0 °C for 2 h, the precipitate was collected by filtration and washed with water. The solid was recrystallized from EtOH−water to give **3q** (1.23 g, 73%) as a colorless crystal, mp 195 °C. ^{1}H NMR (200 MHz, $CDCl_3$) δ: 1.58−1.72 (2H, m), 1.86−1.99 (2H, m), 2.61 (3H, s), 2.63−2.68 (1H, m), 2.81−3.01 (2H, m), 3.14−3.23 (1H, m), 3.46−3.65 (2H, m), 3.97−4.02 (1H, m), 4.13−4.22 (1H, m), 4.25 (2H, s), 4.69−4.74 (1H, m), 6.70 (1H, d, J = 3.3 Hz), 7.59 (1H, dd, J = 8.7 and 2.1 Hz), 7.89−7.96 (4H, m), 8.47 (1H, d, J = 1.5 Hz). Anal. ($C_{24}H_{25}ClN_4O_4S$) C, H, N.

2-(1-{3-[(6-Chloronaphthalen-2-yl)sulfonyl]propanoyl}piperidin-4-yl)-5,7-dimethyl-1,2-dihydro-3*H*-imidazo[1,5-*c*]imidazol-3-one (3r). Compound **3r** was prepared in a manner similar to that described for **3q** in 50% yield as a colorless solid, mp 196−197 °C. ^{1}H NMR (200 MHz, $CDCl_3$) δ: 1.62−1.79 (2H, m), 1.83−1.99 (2H, m), 2.15 (3H, s), 2.57 (3H, s), 2.64−2.71 (1H, m), 2.86−2.99 (2H, m), 3.31−3.26 (1H, m), 3.49−3.63 (2H, m), 3.97−4.18 (4H, m), 4.75−4.96 (1H, m), 7.61 (1H, dd, J = 8.8 and 1.8 Hz), 7.89−7.99 (4H, m), 8.49 (1H, s). Anal. ($C_{25}H_{27}ClN_4O_4S$) C, H, N.

4-Benzyl-*N*-[(2-methyl-1*H*-imidazol-5-yl)methylene]piperazin-1-amine (26). A suspension of **25** (10.0 g, 52.3 mmol) and **22a** (5.80 g, 52.7 mmol) in MeOH (200 mL) was refluxed for 3 h. The reaction mixture was cooled to room temperature and concentrated in vacuo. The residue was triturated with Et_2O to give **26** (13.0 g, 88%) as a pale-yellow solid. ^{1}H NMR (200 MHz, $CDCl_3$) δ: 2.40 (3H, s), 2.62 (4H, t, J = 5.2 Hz), 3.09 (4H, t, J = 5.2 Hz), 3.56 (2H, s), 6.97 (1H, s), 7.24−7.34 (5H, m), 7.43 (1H, s), 9.62 (1H, br s).

4-Benzyl-*N*-[(2-methyl-1*H*-imidazol-5-yl)methyl]piperazin-1-amine (27). To a solution of **26** (13.0 g, 45.9 mmol) in THF (100 mL) was added a solution of borane−THF complex (1 M in THF, 140 mL, 140 mmol) at room temperature. After being stirred at room temperature for 15 h, the reaction mixture was concentrated in vacuo. The residue was dissolved in 6 M HCl, and then the mixture was stirred at 100 °C for 2 h. After cooling to 0 °C, the mixture was basified to pH 12 with 6 M NaOH and extracted with $CHCl_3$. The extract was dried over anhydrous Na_2SO_4 and concentrated in vacuo to give **27** (14.7 g, quantitative) as a brown oil. ^{1}H NMR (200 MHz, $CDCl_3$) δ: 2.37 (3H, s), 2.53 (4H, br s), 2.75 (4H, br s), 3.52 (2H, s), 3.90 (2H, s), 6.76 (1H, s), 7.29−7.32 (5H, m).

2-(4-Benzylpiperazin-1-yl)-5-methyl-1,2-dihydro-3*H*-imidazo[1,5-*c*]imidazol-3-one (28). Compound **28** was prepared in a manner similar to that described for **24a** in 65% yield as a colorless solid. ^{1}H NMR (200 MHz, $CDCl_3$) δ: 2.60−2.65 (7H, m), 3.14 (4H, t, J = 4.6 Hz), 3.55 (2H, s), 4.43 (2H, s), 6.70 (1H, t, J = 2.0 Hz), 7.25−7.34 (5H, m).

5-Methyl-2-(piperazin-1-yl)-1,2-dihydro-3*H*-imidazo[1,5-*c*]imidazol-3-one (29). A suspension of **28** (8.00 g, 25.7 mmol), ammonium formate (16.0 g, 254 mmol), and palladium on carbon (1.60 g) in MeOH (100 mL) was refluxed for 6 h. The mixture was cooled to room temperature, and the insoluble material was filtered off through a Celite pad. The filtrate was concentrated in vacuo, and the residue was triturated with EtOAc and Et_2O to give **29** (5.30 g, 93%) as a pale-yellow solid. ^{1}H NMR (300 MHz, $CDCl_3$) δ: 2.61 (3H, s), 2.98−3.03 (4H, m), 3.10−3.15 (4H, m), 4.44 (2H, s), 6.70 (1H, s).

2-(4-{3-[(6-Chloronaphthalen-2-yl)sulfonyl]propanoyl}piperazin-1-yl)-5-methyl-1,2-dihydro-3*H*-imidazo[1,5-*c*]imidazol-3-one (3s). Compound **3s** was prepared in a manner similar to that described for **3p** in 76% yield as a colorless solid, mp 230−231 °C. ^{1}H NMR (300 MHz, $CDCl_3$) δ: 2.60 (3H, s), 3.13 (2H, t, J = 5.0 Hz), 3.23 (2H, t, J = 5.0 Hz), 3.54−3.59 (4H, m), 3.62 (2H, t, J = 5.0 Hz), 3.69 (2H, t, J = 5.0 Hz), 4.42 (2H, s), 6.70 (1H, t, J = 1.5 Hz), 7.59 (1H, dd, J = 8.6 and 2.3 Hz), 7.89−7.97 (4H, m), 8.47 (1H, s). Anal. ($C_{23}H_{24}ClN_5O_4S$) C, H, N.

In Vitro Assays for the Inhibition of Human FXa. Human FXa (0.3 U/mL) was obtained from Roche Diagnostics. Chromogenic substrate, S-2765 (Chromogenix-Instrumentation Laboratory) was used for the measurement of the inhibition of FXa. Anti-FXa activity was assayed in a buffer containing 50 mM Tris-HCl, 145 mM NaCl, and 2 mM $CaCl_2$ at pH 8.3. Enzyme assay was carried out in 96-well microtiter plates. Test compounds were diluted in DMSO. Compound dilutions and 10 μL of enzyme solution were added to the well containing buffer and preincubated. The enzymatic reactions were initiated with the addition of 10 μL of 3 mM substrate, and the mixture was incubated for 10 min at 37 °C. The reaction was terminated with the addition of 25 μL of 50% acetic acid. The color development from the release of *p*-nitroanilide from each chromogenic substrate was measured at 405 nm on a microtiter plate reader (Multiscan Ascent, Dainippon Sumitomo Pharmaceutical Co.). Each absorbance [T] was calculated by subtracting the absorbance measured without the substrate. The control [C] was performed using DMSO solution in place of test compound. Inhibitory effect (%) was calculated according to the equation (1 − [T]/[C]) × 100. IC_{50} values were calculated by nonlinear regression analysis of the concentration−response curve. Data for new compounds were compared to positive control DX-9065a[6a] (FXa IC_{50} = 0.13 μM). The 95% confidence interval for the IC_{50} of DX-9065a was 0.12−0.15 μM (duplicate).

In Vitro PT Assays. The assay of plasma clotting time was performed using an automatic coagulometer (STA Compact, Diagnostica Stago). PT was measured with STA PT reagents (Roche Diagnostics). An amount of 1.5 μL of compound dilutions in DMSO was added to 48.5 μL of human normal plasma (fresh human plasma, FFP, Sekisui Chemical Co.), and the mixture was preincubated at 37 °C for 4 min. Coagulation was initiated with the addition of 100 μL of thromboplastin, and coagulation time was measured. Coagulation time prolonging ratio (%) was calculated on the basis of coagulation time when DMSO was added instead of test compound. The plasma clotting time doubling concentration (PT_2) was calculated from the regression line based on the method of least squares. Data for new compounds were compared to positive control DX-9065a[6a] (PT_2 = 0.81 ± 0.029 μM (mean ± SEM, n = 3))

Measurement of CYP Inhibition Activity. Inhibition activity of test compounds of CYP3A4 was evaluated by incubating 100 μM testosterone with 10 nM CYP3A4 derived from CYP3A4-expressing human B-lymphoblastoid cells (BD Biosciences) in the presence of 10 μM test compound. The incubation mixture was allowed to stand for 30 min at 37 °C. The concentration of 6β-hydroxytestosterone was measured by HPLC system equipped with a UV detector.

Measurement of ex Vivo PT in Mouse after Oral Administration. Male ICR mice (30−35 g, Clea Japan Inc.) fasting for more than 12 h were employed. Test compounds were orally administered to these animals. An hour after administration, 800 μL of blood was collected from artery abdominal aorta using 3.8% sodium citrate (whole blood/sodium citrate solution = 9:1, v/v), under anesthesia with pentobarbital (50 mg/kg, ip). The citrated blood was centrifuged at 1000*g* for 10 min to obtain platelet poor plasma (PPP). PT was measured with an automatic coagulometer. An amount of 50 μL of PPP was preincubated at 37 °C for 4 min. The PPP was mixed with 100 μL of thromboplastin solution, and then its coagulation time was measured. Test compounds were suspended in 0.5% methyl cellulose (Metolose cp100, Shin-Etsu Chemical), and as control, 0.5% methylcellulose was administered instead of test compounds. Activity of each test compound was shown as a ratio (%) determined by comparing the clotting time of compound-treatment mice with that of control group. We have

validated the ex vivo PT assay for the evaluation of oral bioavailability in mice by use of the positive control compound DX-9065a.[6a] DX-9065a prolonged mouse PT by 1.1-fold at a dose of 30 mg/kg and by 1.4-fold at a dose of 100 mg/kg.

Measurement of ex Vivo PT in Monkey after Oral Administration. Male cynomolgus monkeys (3.5−4 kg, NAFOVANNY) fasting for more than 12 h were employed. Test compounds were orally administered to these animals. After administration, 1.5 mL of blood was collected from the femoral vein using 3.8% sodium citrate (whole blood/sodium citrate solution = 9:1, v/v) at several time points. The citrated blood was centrifuged at 1000*g* for 10 min to obtain PPP. Plasma clotting time and anticoagulating activity of drug were determined as described above.

Enzyme Inhibition Assays. Enzyme assays using chromogenic substrates were performed as follows. Human FXa was obtained from Roche diagnostics. Human thrombin was obtained from Sigma Chemical Co. Human trypsin was obtained from Atheus Research and Technology, Inc. Human plasmin was purchased from BioPur AG. Human t-PA was obtained from Kyowa Hakko Kogyo Co. The chromogenic substrates used were S-2222, S-2366, S-2222, S-2366, S-2302, and S-2288 for FXa, thrombin, trypsin, plasmin, and t-PA, respectively, and obtained from Chromogenix-Instrumentation Laboratory. All enzyme assays were performed at 37 °C in 96-well microtiter plates. The final enzyme concentrations were 0.024 U/mL, 0.080 U/mL, 0.040 μg/mL, 0.040 U/mL, 0.020 U/mL, and 4000 U/mL for FXa, thrombin, trypsin, plasmin, and t-PA, respectively. Compound dilutions were added to the wells containing buffer and enzyme and incubated for 30 min. The enzyme reactions were initiated by the addition of substrate, and the color developed from the release of *p*-nitroanilide from each chromogenic substrate was monitored continuously for 5 min at 405 nm on a microtiter plate reader. The K_i values were determined from a Lineweaver−Burk plot, when the optical densities were measured with different concentrations of substrates.

Pharmacokinetic Analysis in Rats. Test compound was administered to fasted or fed SD (IGS) rats (male, 8 weeks old, $n = 3$) intravenously (0.3 mg/kg, DMA/PEG400) and orally (3 mg/kg, 0.5% methylcellulose suspension). At 5, 10, 15, and 30 min and 1, 2, 4, 8, 24 h after intravenous administration or at 15 and 30 min and 1, 2, 4, 8, 24 h after oral administration, blood samples were collected from tail vein. The blood samples were centrifuged to obtain the plasma fraction. The plasma samples were deproteinized with acetonitrile. After centrifugation, the supernatant obtained was diluted with 0.01 mol/L HCO_2NH_4 (adjusted to pH 3.0 with HCO_2H) and centrifuged again. The compound concentration in the supernatant was measured by LC/MS/MS with an API3000 triple quadrupole mass spectrometer (Perkin-Elmer Sciex). The mass spectrometer was equipped with a turbo ionspray source and operated in positive ion mode. The HPLC conditions were as follows: column, an L-column ODS (2.1 mm × 150 mm); mobile phase, 0.01 mol/L HCO_2NH_4 (adjusted to pH 3.0 with HCO_2H)/acetonitrile = 6/4; flow rate, 0.2 mL/min; column temperature, 40 °C.

Pharmacokinetic Analysis in Cynomolgus Monkeys. Test compound was administered to fasted or fed cynomolgus monkeys (male, $n = 3$) intravenously (0.3 mg/kg, DMA/PEG400) and orally (3 mg/kg, 0.5% methylcellulose suspension). At 5, 10, 15, 30 min and 1, 2, 4, 8, 24 h after intravenous administration or at 15 and 30 min and 1, 2, 4, 8, 24 h after oral administration, blood samples were collected from femoral vein. The blood samples were centrifuged to obtain the plasma fraction. The plasma samples were deproteinized with acetonitrile. After centrifugation, the supernatant obtained was diluted with 0.01 mol/L HCO_2NH_4 (adjusted to pH 3.0 with HCO_2H) and centrifuged again. The compound concentration in the supernatant was measured by LC/MS/MS with an API3000 triple quadrupole mass spectrometer (Perkin-Elmer Sciex). The mass spectrometer was equipped with a turbo ionspray source and operated in positive ion mode. The HPLC conditions were as follows: column, an L-column ODS (2.1 mm × 150 mm); mobile phase, 0.01 mol/L HCO_2NH_4 (adjusted to pH 3.0 with HCO_2H)/acetonitrile = 6/4; flow rate, 0.2 mL/min; column temperature, 40 °C.

Rat Venous Thrombosis Model. Male Sprague−Dawley rats (7 weeks old) were anesthetized with sodium pentobarbital. A 10 mL length of inferior vena cava from the distal region staring the left renal vein was isolated, and any side branches were ligated. A balloon catheter was introduced from the left femoral vein to inferior vena cava to injure the endothelium. Denudation of the endothelium was performed by three passes of the inflated balloon catheter. In order to trigger the thrombus formation at the injured region, a silk thread was tied around the vena cava caudal to the left renal vein with a blunt needle (26 gauge), followed by the removal of the needle. Thirty minutes after the starting of partial stasis, the thrombus formed in the vena cava was removed and the wet weight was measured. Blood samples were collected for the measurement of blood coagulation parameters just after the removal of thrombus. Compound **3q** and warfarin were orally administered 30 min and 18 h, respectively, before inducing the thrombus formation to examine their antithrombotic potency at the points that give maximal anticoagulating effects. Compound **3q** was given after the animals had fasted for more than 12 h.

Measurement of Bleeding Time in Rats after Oral Administration. Male Sprague−Dawley rats (7 weeks old) were anesthetized with sodium pentobarbital. The tail was transected at 2−3 mm proximal site from the tip. Blood was blotted every 30 s with filter paper until either bleeding had stopped or 30 min had elapsed. Compound **3q** and warfarin were orally administered 30 min and 18 h before the measurement of bleeding time, respectively.

Docking Studies. The coordinates of FXa were retrieved from the Protein Data Bank (accession code 1EZQ).[24] Compounds **2**, **3a**, **3i**, **3m**, **3p**, and **3q** were docked into the FXa protein crystal structure using GOLD[23] (version 2.0, the Cambridge Crystallographic Data Centre, U.K.) with the standard default settings. The initial structures of the compounds-complexed FXa models were energy-minimized using the MMFF94s force field in MOE (version 2003.02, Chemical Computing Group, Montreal, Canada) to obtain the final docking models. During the minimization procedure, the following conditions were adopted. The dielectric constant was set to 4*r*, where *r* is the distance between two interacting atoms. The residues, which are 8 Å away from each compound, were fixed. A harmonic force constraint against the initial atomic positions of the backbone was added, using 10 kcal/Å^2 as a force constant. And atomic charges for the protein and the compounds were set according to the AMBER99 force field and the AM1-BCC method, respectively.

Acknowledgment. The authors thank Terufumi Takagi for his docking model study of compounds **3a** and **3q** and helpful discussions; Dr. Teruaki Okuda and Shin-ichi Niwa for carrying out CYP3A4 inhibition measurements for the compounds highlighted in Table 6; Masashi Yamaguchi, Teruki Hamada, and Atsutoshi Furuta for obtaining rat and monkey pharmacokinetic data for compound **3q** in Tables 8 and 9; and Dr. Satoru Asahi, Miyako Sudo, and Naohiro Kawaguchi for carrying out CYP2C8, 2C9, and 2D6 inhibition measurements for compound **3q**.

Supporting Information Available: Elemental analysis data and the binding model of the protonated **3a** in FXa. This material is available free of charge via the Internet at http://pubs.acs.org.

References

(1) Hirsh, J.; Dalen, J. E.; Anderson, D. R.; Poller, L.; Bussey, H.; Ansell, J.; Deykin, D. Oral anticoagulants: mechanism of action, clinical effectiveness, and optimal therapeutic range. *Chest* **2001**, *119*, 8S–21S.

(2) Mann, K. G.; Butenas, S.; Brummel, K. The dynamics of thrombin formation. *Arterioscler., Thromb. Vasc. Biol.* **2003**, *23*, 17–25.

(3) (a) Walenga, J. M.; Jeske, W. P.; Hoppensteadt, D.; Fareed, J. Factor Xa inhibitors: today and beyond. *Curr. Opin. Invest. Drugs* **2003**, *4*, 272–281. (b) Samama, M. M. Synthetic direct and indirect factor Xa

inhibitors. *Thromb. Res.* **2002**, *106*, V267–V273. (c) Kaiser, B. Factor Xa, a promising target for drug development. *Cell. Mol. Life Sci.* **2002**, *59*, 189–192.

(4) (a) Leadley, R. J., Jr. Coagulation factor Xa inhibition: biological background and rationale. *Curr. Top. Med. Chem.* **2001**, *1*, 151–159. (b) Hauptmann, J.; Stürzebecher, J. Synthetic inhibitors of thrombin and factor Xa: from bench to bedside. *Thromb. Res.* **1999**, *93*, 203–241. (c) Wong, P. C.; Crain, E. J.; Watson, C. A.; Zaspel, A. M.; Wright, M. R.; Lam, P. Y.; Pinto, D. J. P.; Wexler, R. R.; Knabb, R. M. Nonpeptide factor Xa inhibitors III: effects of DPC423, an orally-active pyrazole antithrombotic agent, on arterial thrombosis in rabbits. *J. Pharmacol. Exp. Ther.* **2002**, *303*, 993–1000. (d) Wong, P. C.; Pinto, D. J. P.; Knabb, R. M. Nonpeptide factor Xa inhibitors: DPC423, a highly potent and orally bioavailable pyrazole antithrombotic agent. *Cardiovasc. Drug Rev.* **2002**, *20*, 137–152. (e) Perzborn, E.; Strassburger, J.; Wilmen, A.; Pohlmann, J.; Roehrig, S.; Schlemmer, K.-H.; Straub, A. In vitro and in vivo studies of the novel antithrombotic agent BAY 59-7939, an oral, direct factor Xa inhibitor. *J. Thromb. Haemostasis* **2005**, *3*, 514–521.

(5) (a) Al-Obeidi, F.; Ostrem, J. A. Factor Xa inhibitors by classical and combinatorial chemistry. *Drug Discovery Today* **1998**, *3*, 223–231. (b) Adang, A. E. P.; Rewinkel, J. B. M. A new generation of orally active antithrombotics: comparing strategies in the GPIIb/IIIa, thrombin and factor Xa areas. *Drugs Future* **2000**, *25*, 369–383. (c) Alexander, J. H.; Singh, K. P. Inhibition of factor Xa: a potential target for the development of new anticoagulants. *Am. J. Cardiovasc. Drugs* **2005**, *5*, 279–290. (d) Kubitza, D.; Haas, S. Novel factor Xa inhibitors for prevention and treatment of thromboembolic diseases. *Expert Opin. Invest. Drugs* **2006**, *15*, 843–855. (e) Eriksson, B. I.; Quinlan, D. J. Oral anticoagulants in development: focus on thromboprophylaxis in patients undergoing orthopaedic surgery. *Drugs* **2006**, *66*, 1411–1429. (f) Spyropoulos, A. C. Investigational treatments of venous thromboembolism. *Expert Opin. Invest. Drugs* **2007**, *16*, 431–440. (g) Turpie, A. G. G. Oral, direct factor Xa inhibitors in development for the prevention and treatment of thromboembolic diseases. *Arterioscler., Thromb. Vasc. Biol.* **2007**, *27*, 1238–1247. (h) Casimiro-Garcia, A.; Dudley, D. A.; Heemstra, R. J.; Filipski, K. J.; Bigge, C. F.; Edmunds, J. J. Progress in the discovery of factor Xa inhibitors. *Expert Opin. Ther. Pat.* **2006**, *16*, 119–145.

(6) For discussions on various small molecule competitive inhibitors of FXa, see the following: (a) Zhu, B.-Y.; Scarborough, R. M. Recent advances in inhibitors of factor Xa in the prothrombinase complex. *Curr. Opin. Cardiovasc., Pulm. Renal Investig. Drugs* **1999**, *1*, 63–88. (b) Sinha, U. Synthetic inhibitors of coagulation factor Xa. *Expert Opin. Invest. Drugs* **1999**, *8*, 567–573. (c) Al-Obeidi, F.; Ostrem, J. A. Factor Xa inhibitors. *Expert Opin. Ther. Pat.* **1999**, *9*, 931–953. (d) Zhu, B.-Y.; Scarborough, R. M. Factor Xa inhibitors: recent advances in anticoagulant agents. *Annu. Rep. Med. Chem.* **2000**, *35*, 83–102. (e) Rai, R.; Sprengeler, P. A.; Elrod, K. C.; Young, W. B. Perspectives on factor Xa inhibition. *Curr. Med. Chem.* **2001**, *8*, 101–119. (f) Betz, A. Recent advances in factor Xa inhibitors. *Expert Opin. Ther. Pat.* **2001**, *11*, 1007–1017. (g) Quan, M. L.; Smallheer, J. M. The race to an orally active factor Xa inhibitor: recent advances. *Curr. Opin. Drug Discovery Dev.* **2004**, *7*, 460–469.

(7) Roehrig, S.; Straub, A.; Pohlmann, J.; Lampe, T.; Pernerstorfer, J.; Schlemmer, K. H.; Reinemer, P.; Perzborn, E. Discovery of the novel antithrombotic agent 5-chloro-*N*-({(5*S*)-2-oxo-3-[4-(3-oxomorpholin-4-yl)phenyl]-1,3-oxazolidin-5-yl}methyl)thiophene-2-carboxamide (BAY 59-7939): an oral, direct factor Xa inhibitor. *J. Med. Chem.* **2005**, *48*, 5900–5908.

(8) Pinto, D. J. P.; Orwat, M. J.; Koch, S.; Rossi, K. A.; Alexander, R. S.; Smallwood, A.; Wong, P. C.; Rendina, A. R.; Luettgen, J. M.; Knabb, R. M.; He, K.; Xin, B.; Wexler, R. R.; Lam, P. Y. S. Discovery of 1-(4-methoxyphenyl)-7-oxo-6-(4-(2-oxopiperidin-1-yl)phenyl)-4,5,6,7-tetrahydro-1*H*-pyrazolo[3,4-*c*]pyridine-3-carboxamide (Apixaban, BMS-562247), a highly potent, selective, efficacious, and orally bioavailable inhibitor of blood coagulation factor Xa. *J. Med. Chem.* **2007**, *50*, 5339–5356.

(9) Imaeda, Y.; Kawamoto, T.; Tobisu, M.; Konishi, N.; Hiroe, K.; Kawamura, M.; Tanaka, T.; Kubo, K. Discovery of piperazinylimidazo[1,2-*a*]pyridines as novel S4 binding elements for orally active factor Xa inhibitors. *Bioorg. Med. Chem.* **2008**, *16*, 3125–3140.

(10) Quan, M. L.; Lam, P. Y. S.; Han, Q.; Pinto, D. J. P.; He, M. Y.; Li, R.; Ellis, C. D.; Clark, C. G.; Teleha, C. A.; Sun, J.-H.; Alexander, R. S.; Bai, S.; Luettgen, J. M.; Knabb, R. M.; Wong, P. C.; Wexler, R. R. Discovery of 1-(3′-aminobenzisoxazol-5′-yl)-3-trifluoromethyl-*N*-[2-fluoro-4-[(2′-dimethylaminomethyl)imidazol-1-yl]phenyl]-1*H*-pyrazole-5-carboxyamide hydrochloride (razaxaban), a highly potent, selective, and orally bioavailable factor Xa inhibitor. *J. Med. Chem.* **2005**, *48*, 1729–1744.

(11) (a) Brandstetter, H.; Kühne, A.; Bode, W.; Huber, R.; von der Saal, W.; Wirthensohn, K.; Engh, R. A. X-ray structure of active site-inhibited clotting factor Xa. Implications for drug design and substrate recognition. *J. Biol. Chem.* **1996**, *271*, 29988–29992. (b) Haginoya, N.; Kobayashi, S.; Komoriya, S.; Yoshino, T.; Suzuki, M.; Shimada, T.; Watanabe, K.; Hirokawa, Y.; Furugori, T.; Nagahara, T. Synthesis and conformational analysis of a non-amidine factor Xa inhibitor that incorporates 5-methyl-4,5,6,7-tetrahydrothiazolo[5,4-*c*]pyridine as S4 binding element. *J. Med. Chem.* **2004**, *47*, 5167–5182.

(12) Kubo, K.; Kuroita, T.; Imaeda, Y.; Kawamura, M. Imidazole Derivative, Process for Producing the Same, and Use. WO 2004/048363, 2004; *Chem. Abstr.* **2004**, *141*, 38631.

(13) Kim, D.; Wang, L.; Hale, J. J.; Lynch, C. L.; Budhu, R. J.; MacCoss, M.; Mills, S. G.; Malkowitz, L.; Gould, S. L.; DeMartino, J. A.; Springer, M. S.; Hazuda, D.; Miller, M.; Kessler, J.; Hrin, R. C.; Carver, G.; Carella, A.; Henry, K.; Lineberger, J.; Schleif, W. A.; Emini, E. A. Potent 1,3,4-trisubstituted pyrrolidine CCR5 receptor antagonists: effects of fused heterocycles on antiviral activity and pharmacokinetic properties. *Bioorg. Med. Chem. Lett.* **2005**, *15*, 2129–2134.

(14) Imaeda, Y.; Miyawaki, T.; Sakamoto, H.; Itoh, F.; Konishi, N.; Hiroe, K.; Kawamura, M.; Tanaka, T.; Kubo, K. Discovery of sulfonylalkylamides: a new class of orally active factor Xa inhibitors. *Bioorg. Med. Chem.* **2008**, *16*, 2243–2260.

(15) Lange, J. H. M.; Wals, H. C.; van den Hoogenband, A.; van de Kuilen, A.; den Hartog, J. A. J. Two novel syntheses of the histamine H_3 antagonist thioperamide. *Tetrahedron* **1995**, *51*, 13447–13454.

(16) Bordi, F.; Mor, M.; Plazzi, P. V.; Silva, C.; Morini, G.; Caretta, A.; Barocelli, E.; Impicciatore, M. Synthesis and binding assays of H3-receptor ligands. *Farmaco* **1992**, *47*, 1343–1365.

(17) Greengrass, C. W.; Street, S. D. A.; Whittle, P. J. Preparation of Antiviral Peptide Analogs. WO 93/19059, 1993; *Chem. Abstr.* **1993**, *121*, 256333.

(18) (a) Siegel, M. G.; Chaney, M. O.; Bruns, R. F.; Clay, M. P.; Schober, D. A.; Van Abbema, A. M.; Johnson, D. W.; Cantrell, B. E.; Hahn, P. J.; Hunden, D. C.; Gehlert, D. R.; Zarrinmayeh, H.; Ornstein, P. L.; Zimmerman, D. M.; Koppel, G. A. Rapid parallel synthesis applied to the optimization of a series of potent nonpeptide neuropeptide Y-1 receptor antagonists. *Tetrahedron* **1999**, *55*, 11619–11639. (b) Egbertson, M. S.; Chang, C. T.-C.; Duggan, M. E.; Gould, R. J.; Halczenko, W.; Hartman, G. D.; Laswell, W. L.; Lynch, J. J., Jr.; Lynch, R. J.; Manno, P. D.; Naylor, A. M.; Prugh, J. D.; Ramjit, D. R.; Sitko, G. R.; Smith, R. S.; Turchi, L. M.; Zhang, G. Non-peptide fibrinogen receptor antagonists. 2. Optimization of a tyrosine template as a mimic for Arg-Gly-Asp. *J. Med. Chem.* **1994**, *37*, 2537–2551.

(19) An, H.; Wang, T.; Mohan, V.; Griffey, R. H.; Dan Cook, P. Solution phase combinatorial chemistry. Discovery of 13- and 15-membered polyazapyridinocyclophane libraries with antibacterial activity. *Tetrahedron* **1998**, *54*, 3999–4012.

(20) The log *D* values were determined at pH 7.4 as indicated in the following: Yamagami, C.; Ogura, T.; Takao, N. Hydrophobicity parameters determined by reversed-phase liquid chromatography I. Relationship between capacity factors and octanol−water partition coefficients for monosubstituted pyrazines and the related pyridines. *J. Chromatogr.* **1990**, *514*, 123–136.

(21) The pK_a values were determined by use of an automatic titrator (Hiranuma COM-2500). A 10 mL portion of a compound solution, approximately 0.4 mg/mL compound with 0.1 mL of 0.1 M HCl added, was used. Blank consisted of 10 mL of 1 mM HCl. The titration was carried out using microliter amounts of 0.1 M NaOH.

(22) Good correlation between log *D* and in vitro anticoagulant activity has been recently reported: (a) Hirayama, F.; Koshio, H.; Katayama, N.; Kurihara, H.; Taniuchi, Y.; Sato, K.; Hisamichi, N.; Sakai-Moritani, Y.; Kawasaki, T.; Matsumoto, Y.; Yanagisawa, I. The discovery of YM-60828: a potent, selective and orally-bioavailable factor Xa inhibitor. *Bioorg. Med. Chem.* **2002**, *10*, 1509–1523. (b) Chan, C.; Borthwick, A. D.; Brown, D.; Burns-Kurtis, C. L.; Campbell, M.; Chaudry, L.; Chung, C.; Convery, M. A.; Hamblin, J. N.; Johnstone, L.; Kelly, H. A.; Kleanthous, S.; Patikis, A.; Patel, C.; Pateman, A. J.; Senger, S.; Shah, G. P.; Toomey, J. R.; Watson, N. S.; Weston, H. E.; Whitworth, C.; Young, R. J.; Zhou, P. Factor Xa inhibitors: S1 binding interactions of a series of *N*-{(3*S*)-1-[(1*S*)-1-methyl-2-morpholin-4-yl-2-oxoethyl]-2-oxopyrrolidin-3-yl}sulfonamides. *J. Med. Chem.* **2007**, *50*, 1546–1557. (c) Zhang, P.; Bao, L.; Zuckett, J. F.; Goldman, E. A.; Jia, Z. J.; Arfsten, A.; Edwards, S.; Sinha, U.; Hutchaleelaha, A.; Park, G.; Lambing, J. L.; Hollenbach, S. J.; Scarborough, R. M.; Zhu, B.-Y. Design, synthesis, and SAR of anthranilamide-based factor Xa inhibitors incorporating substituted biphenyl P4 motifs. *Bioorg. Med. Chem. Lett.* **2004**, *14*, 983–987. (d) Masters, J. J.; Franciskovich, J. B.; Tinsley, J. M.; Campbell, C.; Campbell, J. B.; Craft, T. J.; Froelich, L. L.; Gifford-Moore, D. S.; Hay, L. A.; Herron, D. K.; Klimkowski, V. J.; Kurz, K. D.; Metz, J. T.; Ratz, A. M.; Shuman, R. T.; Smith, G. F.; Smith, T.; Towner, R. D.; Wiley, M. R.; Wilson, A.; Yee, Y. K. Non-amidine-containing 1,2-dibenzamidobenzene inhibitors of human factor Xa with potent anticoagulant and antithrombotic activity. *J. Med. Chem.* **2000**, *43*, 2087–2092. (e) Chou,

Y.-L.; Davey, D. D.; Eagen, K. A.; Griedel, B. D.; Karanjawala, R.; Phillips, G. B.; Sacchi, K. L.; Shaw, K. J.; Wu, S. C.; Lentz, D.; Liang, A. M.; Trinh, L.; Morrissey, M. M.; Kochanny, M. J. Structure−activity relationships of substituted benzothiophene−anthranilamide factor Xa inhibitors. *Bioorg. Med. Chem. Lett.* **2003**, *13*, 507–511. (f) Kochanny, M. J.; Adler, M.; Ewing, J.; Griedel, B. D.; Ho, E.; Karanjawala, R.; Lee, W.; Lentz, D.; Liang, A. M.; Morrissey, M. M.; Phillips, G. B.; Post, J.; Sacchi, K. L.; Sakata, S. T.; Subramanyam, B.; Vergona, R.; Walters, J.; White, K. A.; Whitlow, M.; Ye, B.; Zhao, Z.; Shaw, K. J. Substituted thiophene−anthranilamides as potent inhibitors of human factor Xa. *Bioorg. Med. Chem.* **2007**, *15*, 2127–2146. (g) Zhang, P.; Bao, L.; Zuckett, J. F.; Jia, Z. J.; Woolfrey, J.; Arfsten, A.; Edwards, S.; Sinha, U.; Hutchaleelaha, A.; Lambing, J. L.; Hollenbach, S. J.; Scarborough, R. M.; Zhu, B.-Y. Design, synthesis, and SAR of anthranilamide-based factor Xa inhibitors with improved functional activity. *Bioorg. Med. Chem. Lett.* **2004**, *14*, 989–993. (h) Tucker, T. J.; Lumma, W. C.; Lewis, S. D.; Gardell, S. J.; Lucas, B. J.; Baskin, E. P.; Woltmann, R.; Lynch, J. J.; Lyle, E. A.; Appleby, S. D.; Chen, I-W.; Dancheck, K. B.; Vacca, J. P. Potent noncovalent thrombin inhibitors that utilize the unique amino acid D-dicyclohexylalanine in the P3 position. Implications on oral bioavailability and antithrombotic efficacy. *J. Med. Chem.* **1997**, *40*, 1565–1569. (i) Tucker, T. J.; Brady, S. F.; Lumma, W. C.; Lewis, S. D.; Gardell, S. J.; Naylor-Olsen, A. M.; Yan, Y.; Sisko, J. T.; Stauffer, K. J.; Lucas, B. J.; Lynch, J. J.; Cook, J. J.; Stranieri, M. T.; Holahan, M. A.; Lyle, E. A.; Baskin, E. P.; Chen, I.-W.; Dancheck, K. B.; Krueger, J. A.; Cooper, C. M.; Vacca, J. P. Design and synthesis of a series of potent and orally bioavailable noncovalent thrombin inhibitors that utilize nonbasic groups in the P1 position. *J. Med. Chem.* **1998**, *41*, 3210–3219. (j) Ye, B.; Arnaiz, D. O.; Chou, Y.-L.; Griedel, B. D.; Karanjawala, R.; Lee, W.; Morrissey, M. M.; Sacchi, K. L.; Sakata, S. T.; Shaw, K. J.; Wu, S. C.; Zhao, Z.; Adler, M.; Cheeseman, S.; Dole, W. P.; Ewing, J.; Fitch, R.; Lentz, D.; Liang, A.; Light, D.; Morser, J.; Post, J.; Rumennik, G.; Subramanyam, B.; Sullivan, M. E.; Vergona, R.; Walters, J.; Wang, Y.-X.; White, K. A.; Whitlow, M.; Kochanny, M. J. Thiophene−anthranilamides as highly potent and orally available factor Xa inhibitors. *J. Med. Chem.* **2007**, *50*, 2967–2980.

(23) Jones, G.; Willett, P.; Glen, R. C.; Leach, A. R.; Taylor, R. Development and validation of a genetic algorithm for flexible docking. *J. Mol. Biol.* **1997**, *267*, 727–748.

(24) Maignan, S.; Guilloteau, J.-P.; Pouzieux, S.; Choi-Sledesky, Y. M.; Becker, M. R.; Klein, S. I.; Ewing, W. R.; Pauls, H. W.; Spada, A. P.; Mikol, V. Crystal structures of human factor Xa complexed with potent inhibitors. *J. Med. Chem.* **2000**, *43*, 3226–3232.

(25) The tetrahydroimidazo[1,2-*a*]pyridine ring of compound **3a** would be protonated at physiological pH. The docking model of the protonated compound **3a** showed a binding mode highly similar to that of the base **3a** in Figure 2. The docking model of the protonated compound **3a** in FXa is available in the Supporting Information.

(26) Veber, D. F.; Johnson, S. R.; Cheng, H.-Y.; Smith, B. R.; Ward, K. W.; Kopple, K. D. Molecular properties that influence the oral bioavailability of drug candidates. *J. Med. Chem.* **2002**, *45*, 2615–2623.

(27) Lam, P. Y. S.; Clark, C. G.; Li, R.; Pinto, D. J. P.; Orwat, M. J.; Galemmo, R. A.; Fevig, J. M.; Teleha, C. A.; Alexander, R. S.; Smallwood, A. M.; Rossi, K. A.; Wright, M. R.; Bai, S. A.; He, K.; Luettgen, J. M.; Wong, P. C.; Knabb, R. M.; Wexler, R. R. Structure-based design of novel guanidine/benzamidine mimics: potent and orally bioavailable factor Xa inhibitors as novel anticoagulants. *J. Med. Chem.* **2003**, *46*, 4405–4418.

(28) (a) Gonzalez, F. J. The molecular biology of cytochrome P450s. *Pharmacol. Rev.* **1988**, *40*, 243–288. (b) Dresser, G. K.; Spence, J. D.; Bailey, D. G. Pharmacokinetic−pharmacodynamic consequences and clinical relevance of cytochrome P450 3A4 inhibition. *Clin. Pharmacokinet.* **2000**, *38*, 41–57. (c) Wrighton, S. A.; Schuetz, E. G.; Thummel, K. E.; Shen, D. D.; Korzekwa, K. R.; Watkins, P. B. The human CYP3A subfamily: practical considerations. *Drug Metab. Rev.* **2000**, *32*, 339–361.

(29) For a discussion on the importance of enzyme binding selectivity, see the following: (a) Wiley, M. R.; Chirgadze, N. Y.; Clawson, D. K.; Craft, T. J.; Gifford-Moore, D. S.; Jones, N. D.; Olkowski, J. L.; Schacht, A. L.; Weir, L. C.; Smith, G. F. Serine protease selectivity of the thrombin inhibitor D-Phe-Pro-agmatine and its homologs. *Bioorg. Med. Chem. Lett.* **1995**, *5*, 2835–2840. (b) Pruitt, J. R.; Pinto, D. J. P.; Galemmo, R. A., Jr.; Alexander, R. S.; Rossi, K. A.; Wells, B. L.; Drummond, S.; Bostrom, L. L.; Burdick, D.; Bruckner, R.; Chen, H.; Smallwood, A.; Wong, P. C.; Wright, M. R.; Bai, S.; Luettgen, J. M.; Knabb, R. M.; Lam, P. Y. S.; Wexler, R. R. Discovery of 1-(2-aminomethylphenyl)-3-trifluoromethyl-*N*-[3-fluoro-2′-(aminosulfonyl)[1,1′-biphenyl]]-4-yl]-1*H*-pyrazole-5-carboxyamide (DPC602), a potent, selective, and orally bioavailable factor Xa inhibitor. *J. Med. Chem.* **2003**, *46*, 5298–5315.

(30) CYP2C8 and 2C9 inhibitory activities were determined by a reported method. See the following: Miners, J. O.; Smith, K. J.; Robson, R. A.; McManus, M. E.; Veronese, M. E.; Birkett, D. J. Tolbutamide hydroxylation by human liver microsomes: kinetic characterisation and relationship to other cytochrome P-450 dependent xenobiotic oxidations. *Biochem. Pharmacol.* **1988**, *37*, 1137–1144.

(31) CYP2D6 inhibitory activity was determined by a reported method. See the following: Kronbach, T.; Mathys, D.; Gut, J.; Catin, T.; Meyer, U. A. High-performance liquid chromatographic assay for bufuralol 1′-hydroxylase, debrisoquine 4-hydroxylase, and dextromethorphan *O*-demethylase in microsomes and purified cytochrome P-450 isozymes of human liver. *Anal. Biochem.* **1987**, *162*, 24–32.

(32) (a) Pauls, H. W.; Ewing, W. R. The design of competitive, small-molecule inhibitors of coagulation factor Xa. *Curr. Top. Med. Chem.* **2001**, *1*, 83–100. (b) Adler, M.; Kochanny, M. J.; Ye, B.; Rumennik, G.; Light, D. R.; Biancalana, S.; Whitlow, M. Crystal structures of two potent nonamidine inhibitors bound to factor Xa. *Biochemistry* **2002**, *41*, 15514–15523. (c) Maignan, S.; Guilloteau, J.-P.; Choi-Sledeski, Y. M.; Becker, M. R.; Ewing, W. R.; Pauls, H. W.; Spada, A. P.; Mikol, V. Molecular structures of human factor Xa complexed with ketopiperazine inhibitors: preference for a neutral group in the S1 pocket. *J. Med. Chem.* **2003**, *46*, 685–690. (d) Nazaré, M.; Will, D. W.; Matter, H.; Schreuder, H.; Ritter, K.; Urmann, M.; Essrich, M.; Bauer, A.; Wagner, M.; Czech, J.; Lorenz, M.; Laux, V.; Wehner, V. Probing the subpockets of factor Xa reveals two binding modes for inhibitors based on a 2-carboxyindole scaffold: a study combining structure−activity relationship and X-ray crystallography. *J. Med. Chem.* **2005**, *48*, 4511–4525.

(33) (a) Galemmo, R. A., Jr.; Wells, B. L.; Rossi, K. A.; Alexander, R. S.; Dominguez, C.; Maduskuie, T. P.; Stouten, P. F. W.; Wright, M. R.; Aungst, B. J.; Wong, P. C.; Knabb, R. M.; Wexler, R. R. The de novo design and synthesis of cyclic urea inhibitors of factor Xa: optimization of the S4 ligand. *Bioorg. Med. Chem. Lett.* **2000**, *10*, 301–304. (b) Maignan, S.; Mikol, V. The use of 3D structural data in the design of specific factor Xa inhibitors. *Curr. Top. Med. Chem.* **2001**, *1*, 161–174.

JM701548U